Spatial and temporal variation of CO over Alberta using measurements from satellite, aircrafts, and ground stations

Heba S Marey[1,2], Zaher Hashisho[1], Long Fu[3] and John Gille[4]

[1] University of Alberta, Department of Civil and Environmental Engineering, Edmonton, Alberta, Canada

[2] Alexandria University, Institute of Graduate Studies and Research, Alexandria, Egypt.

[3] Alberta Environment and Sustainable Resource Development, Environmental Monitoring, Alberta, Canada

[4] National Center for Atmospheric Research, Boulder, Colorado, USA.

Abstract

Alberta is Canada's largest oil producer and its oil sand deposits comprise 30% of the world's oil reserves. The process of bitumen extraction and upgrading releases trace gases and aerosols to the atmosphere. In this study we present satellite-based analysis to explore, for the first time, various contributing factors that affect tropospheric carbon monoxide (CO) levels over Alberta. The multispectral product that uses both near-infrared (NIR) and the thermal-infrared (TIR) radiances for CO retrieval from the Measurements of Pollution in the Troposphere (MOPITT) are examined for the 12 year period from 2002–2013. Moderate Resolution Imaging Spectroradiometer (MODIS) thermal anomaly product from 2001 to 2013 is employed to investigate the seasonal and temporal variations of forest fires. Additionally, in-situ CO measurements at industrial and urban sites are compared to satellite data. Furthermore, the available MOZAIC/IAGOS (Measurement of Ozone, Water Vapor, Carbon Monoxide, Nitrogen Oxide by Airbus In-Service Aircraft/In service Aircraft for Global Observing System) aircraft CO profiles (April 2009-December 2011) are used to validate MOPITT CO data. The climatological time curtain plot and spatial maps for CO over northern Alberta indicate the signatures of transported CO for two distinct biomass burning seasons, summer and spring. Distinct seasonal patterns of CO at the urban sites (Edmonton and Calgary cities) point to the strong influence of traffic. Meteorological parameters play an important role on the CO spatial distribution at various pressure levels. Northern Alberta shows stronger upward lifting motion which leads to larger CO total column values while the poor dispersion in central and south Alberta exacerbates the surface CO pollution. Inter-annual variations of satellite data depict a slightly decreasing trend for both regions while the decline trend is more evident from ground observations, especially at the urban sites. MOPITT CO vertical averages and MOZAIC/IAGOS aircraft profiles were in good agreement within the standard deviations at all pressure levels. There is consistency between the time evolution of high CO episodes monitored by satellite and ground measurements and the fire frequency peak time which implies that biomass burning has affected the tropospheric CO distribution in northern Alberta. These findings have further demonstrated the potential use of MOPITT V5 multispectral (NIR+TIR) product for assessing a complicated surface process.

1 Introduction

Canada's crude oil reserves represent the world's 3rd largest after Saudi Arabia and are currently the world's 7th largest producer of crude oil (CAPP, 2012). Alberta is Canada's largest oil producer and its oil sands deposits comprise 30% of the world's oil reserves (Kean, 2009). Alberta's oil sands deposits are located in three regions: Athabasca, Peace River and Cold Lake. The Athabasca oil sands region (AOSR) (Fig. 1) contains most of the oil sands reserves. About 20% of the deposits in the Athabasca region are shallow (<75m deep) and hence can be surface mined. The bitumen contained within the sand is extremely heavy crude oil, requiring heat or solvents to extract it from the sand (Alberta Environment, 2012). The surface mining of the bitumen utilizes a hot water process for extraction, which releases SO_2, H_2S and light hydrocarbons as well as CO_2 and CO (Strausz et al., 1977). After extraction, water and solids are removed from bitumen using solvents/diluents such as naphtha (Siddique et al., 2007) and Paraffins (Siddique et al., 2006) which are also used to decrease the bitumen's viscosity so that it can be ready for processing. Deeper deposits are not recoverable by surface mining: in-situ recovery methods such as steam injection are needed for extraction. Large amounts of natural gas are required to upgrade the bitumen before it is sent through pipelines (NEB, 2013). Thus the rapid expansion of oil extraction, and massive energy requirements to extract and upgrade the bitumen, led to numerous environmental concerns, particularly on air quality (Timoney, and Lee, 2009) and hence an environmental monitoring program that measures the ambient air quality is needed. Air monitoring in Alberta is carried out through airshed associations that were launched as non-profit societies under the umbrella of the Clean Air Strategic Alliance (CASA). Air quality in the AOSR is monitored locally by the Wood Buffalo Environmental Association (WBEA), which is a multi-stakeholder organization (WBEA, 2013). In addition to the existing continuous air quality monitoring network in Alberta, independents studies were conducted to investigate the impact of the oil sands mining operations on the air quality over Alberta (e.g. Bytnerowicz et. al., 2010; Jacob et al., 2010; Simpson et. al., 2010; Howell et al., 2014). Recent studies of aerosol and trace gas emissions have been carried out in summer 2008 when the NASA DC-8 and P-3B research aircraft were deployed at the Canadian Forces Base Cold Lake in Alberta, Canada (Jacob et al., 2010). Their work reported significantly elevated levels of trace gases (CO_2, CH_4, CO, NO, NO_2, NOy, SO_2 and 53 VOCs) above background levels (Simpson et

al. 2010). However, these data are limited in spatial coverage as they reflect local air quality and cannot provide information about the overall regional air quality. A complementary approach to surface and aircraft measurements is satellite-based monitoring which can provide large spatial coverage and making measurements over extended periods of time, allowing the study of the impact of intense emission sources on regional and global scale air quality. Over the last decade, satellite remote sensing of trace gases and aerosols for air quality applications has progressed (Martin, 2008). Despite the emerging importance of using satellite in air quality applications, there has been no studies published using them over Alberta until 2012, when McLinden et. al. (2012) employed the Ozone Monitoring Instrument (OMI) instrument for NO_2 and SO_2 assessment over the AOSR. They presented high-resolution maps that revealed distinct increases above background levels for both species over the area of intensive surface mining. In addition, they showed that NO_2 is increasing at a rate of 11%/year which is generally consistent with the annual rate increase of bitumen production. Accordingly, further study to characterize more trace gases and aerosols that are emitted from various natural and anthropogenic sources in Alberta is required.

Beside oil sands operations, Alberta has other anthropogenic sources, such as combustion of fossil fuels and various industrial processes which emit 428,692.5 tonnes of CO in 2012(EC, 2012). Additionally, natural emissions such as boreal forest fires are a major source of CO. Canada boreal forest fires in summer influence the carbon cycle (Preston and Schmidt, 2006), climate (Amiro et al., 2001), and air quality (Colarco et al., 2004; Pfister et al., 2006). The fire frequency at high latitudes (>55◦ N), is expected to increase (Gillett et al., 2004; Girardin, 2007) as a result of global warming (Stocks et al., 1998; Flannigan et al., 2005) which is accompanied by increased dryness and temperature (Marlon et al., 2008).

One of the most important trace gases emitted from anthropogenic pollution and open biomass burning, is CO. CO can also be produced from photochemical oxidation of CH_4 and non-methane hydrocarbons (Novelli et al., 1998; Duncan et al., 2007). CO plays a critical role in the tropospheric chemistry where it is the dominant sink of the hydroxyl radical (OH), which is the major oxidizing agent in the troposphere. It has also impacts on regional air quality where it can be a precursor to photochemical ozone smog in areas with sufficient NO_x (Ridley et al., 1992). Additionally, CO was recognized as an important indirect greenhouse gas that could have

an effect on global climate (Daniel and Solomon, 1998). With a relatively long life-time (the global average CO lifetime is about 2 months), CO is an excellent tracer for tropospheric transport processes (Pétron, 2004) and plumes from strong emission sources that are extending great distances. Fortunately, CO is one of the few tropospheric gases that can be successfully monitored from space at the present time. It has been measured by the Measurements of Pollution in the Troposphere (MOPITT) instrument on NASA's Terra satellite, creating a global record from 2000 to the present. Thus, the long term record of MOPITT data allows the investigation of the inter-annual and spatial variability of tropospheric CO air quality. Accordingly the current study aims to address the general features of the overall CO loading over Alberta using MOPITT data. The major source contributions of CO and their impacts on temporal and spatial variability will be examined through the use of MOPITT and Moderate Resolution Imaging Spectroradiometer (MODIS) sensors, meteorology and ground level measurements. This work is the first study to explore various contributing factors that affect tropospheric CO levels over Alberta using satellite remote sensing observations. The data and methods used in the study are described briefly. Climatological spatial distribution and time-altitude profiles of MOPITT CO over Alberta are presented and compared with aircraft CO profiles and ground-level measurements. The contribution of forest fires to CO levels in the AOSR are analysed using MODIS fire counts.

2 Data and Methods

This study uses data from two satellite instruments, MODIS (available from https://earthdata.nasa.gov/data/near-real-time-data/firms) and MOPITT V5J (available from ftp://l5eil01.larc.nasa.gov/MOPITT/MOP02J.005) coupled with ground measurement data (available from http://www.casadata.org/). Fort McMurray, Edmonton, and Calgary areas are chosen for analysis where the former represents an industrial oil sand region and the latter represents an urban region. The boundaries of the study areas are:

Fort McMurray	56.0 to 58.0N	112.0 to 110.0W
Edmonton	52.0 to 54.0N	114.0 to 112.0W
Calgary	50.0 to 52.0N	115.0 to 113.0W

2.1 Satellite Data

2.1.1 MOPITT

The MOPITT instrument on board Terra spacecraft is specifically designed to measure CO profiles and total columns (Drummond, 1992). It takes about 3 days for near-complete global coverage with a horizontal resolution of 22 km×22 km at nadir (Deeter et al., 2003). MOPITT has a unique feature compared to other tropospheric CO satellite instruments, as it measures CO simultaneously in both the thermal infrared (TIR) band (4.7 µm) and the near-infrared (NIR) band (2.3 µm). The NIR observations mainly provide information about the CO total column whereas TIR radiances are often most sensitive to CO in the middle and upper-troposphere. In this study we used the MOPITT multispectral product that exploits both channels (TIR+ NIR) which has been shown to have higher sensitivity to CO in the lower troposphere (Worden et al., 2010; Deeter et al., 2011, 2012; Jiang et al., 2013). MOPITT V5 data have been recently validated using in situ CO profiles measured from aircraft (Deeter et al., 2013). Only daytime MOPITT retrievals were used in this study because the NIR channels operate by reflected sunlight and so at night the TIR+NIR product is identical to the TIR product that has no sensitivity near the surface.

2.1.2 **MODIS thermal anomaly products.**

MODIS sensors are located on the Terra and Aqua satellite platforms. They were designed to offer a broad range of information about land, oceanic, and atmospheric conditions (Kaufman et al., 1998a and Masuoka et al., 1998). They detect fires globally on a daily basis at 1 km spatial resolution. The fire detection algorithm has been described by Kaufman et al. (1998b) and Giglio et al. (2003). In this study we used the Collection 5.1 Terra and Aqua MODIS MOD1/MYD14 product from November 2000 (Terra) and July 2002 (Aqua) through December 2012. Each fire pixel is associated with a confidence limit parameter to specify the quality of the data which range from 0% to 100% (Giglio, 2007). The threshold limit for fire pixel confidence that is used in this study is 30%, which is a heuristic measure of the radiometric contrast between a fire pixel

and its immediate non-fire neighborhood, with extra penalties imposed near potential false alarm sources such as cloud edges and coastlines (Giglio et al., 2003). We used the MODIS fire data in the shape file format in order to use them in geographic information system (GIS) maps. Data were obtained from the Land Atmosphere Near-real time Capability for EOS (LANCE) system operated by the NASA/GSFC/Earth Science Data.

2.2 **CASA Ground** Measurements

The CASA Data Warehouse (www.casadata.org) is a central repository for ambient air quality data collected in Alberta. The in-situ measurements of surface CO were recorded at nine monitoring stations in the study region. CO is monitored continuously either by non-dispersive infrared photometry or gas filter correlation (Alberta Environment, 2013). The stations in Edmonton and Calgary are part of the monitoring network in typical urban centres, however Fort McMurray station represents industrial region.

2.3 MOZAIC/IAGOS (Measurement of Ozone, Water Vapor, Carbon Monoxide, Nitrogen Oxide by Airbus In-Service Aircraft/In service Aircraft for Global Observing System) Aircraft Measurements

IAGOS (formerly MOZAIC) instruments onboard commercial aircraft since August 1994, aim to sample the tropospheric gases with high vertical resolution over about 50 airports (Marenco et al., 1998). CO has been monitored since 2001 using the infrared CO analyzer (Model 48CTL from Thermo Environmental Instruments, USA) with a precision of ±5 ppbv (Nedelec et al., 2003). Data are available at http://www.iagos.org.

2.4 Meteorological Data and HYSPLIT Trajectories

The HYSPLIT (Hybrid Single-Particle Lagrangian Integrated Trajectory) model Version 4 was used to generate air mass backward trajectories. It is the latest version of an integrated system for computing air parcel trajectories, dispersion and deposition simulations. The model calculates the trajectories using the Global Data Assimilation System (GDAS) meteorological dataset which has been operated by National Centers for Environmental Prediction (NCEP) (Rolph and Rolph, 2013; Draxler et al., 2013). Trajectory calculation is carried out by time integration of the position of an air parcel as it is transported by the 3-D winds (Draxler and Hess, 1998). Data of mean monthly omega for the study period were taken from the National

Oceanic and Atmospheric Administration (NOAA) Climate Data Assimilation System I, based on the National Centers for Environmental Prediction/National Center for Atmospheric Research (NCEP/NCAR) Reanalysis Project. The NCEP/NCAR global re-analysis meteorological dataset is described in detail by Kalnay et al. (1996).

3 Results and Discussion

3.1 Climatological Spatial Distribution of MOPITT CO over Alberta

Figure 2 shows the seasonally averaged distribution of MOPITT CO total column measurements over Alberta for the period March 2002 to December 2013. The symbols F, E and C represent the cities of Fort McMurray, Edmonton and Calgary, respectively. Data are gridded at 0.25x0.25 degree resolution. Figure 2 depicts the seasonal climatological maps for CO total columns. High CO loadings extended from the North East to North West of Alberta in all seasons except in fall (December-February) where the spatial variations are less prominent (the flattest distribution). CO total columns illustrate remarkable maximum values in the northeast area (oil sand area) in the spring (March-May) where the CO total column ranges are 2.5-2.75 x 10^18 molecules cm^{-2}. Additionally, it is apparent that summer (June-August) and fall (September-November) seasons display minimum CO loading, especially in central and southern Alberta.

The spatial distributions of CO mixing ratios at the surface level (Figure 3) reveal distinct enhancements, covering south east Alberta in winter with CO mixing ratios of 180-200 ppb. In the spring the CO mixing ratios are generally high in the whole of Alberta. The summer season demonstrates relatively high surface CO concentrations (140-160 ppb) north of Fort McMurray, although it shows minimum levels for the rest of Alberta, while the fall season illustrates distinctly flatter spatial distribution. Thus, the spatial distributions of surface CO especially in spring indicate a different pattern than the CO total column (Figure 2) for the same period. To assist in the interpretation of the results, the vertical velocity (Omega) which is defined as change of pressure with time is analyzed. The spatial distributions of averaged Omega (dp/dt) for 2002-2013 at pressure level 850 mb for four seasons are depicted in Figure 4. They demonstrate upward movements of air mass in the area of northeast and southwest of Alberta as indicated by negative values. This suggests that the CO emissions are uplifted, raising the CO total column

values in the north area. Conversely, downward movements (positive values) are recorded in the center and south east Alberta allowing subsidence of CO emissions as conditions are favorable. Therefore, there is a general consistency between the climatological maps of Omega and the CO spatial distributions where the CO total columns shows remarkable enhancements in the north while the surface CO experiences elevated values in the south area. This highlights the important role of meteorological parameters on ambient air quality.

The southwestern area of Alberta exhibits minimum CO levels, which are less than 1.5 x 10^18 molecule/cm^2 and 60 ppb for CO total column and surface concentration (Figure 2 and Figure 3), respectively. Alberta has a varied topography, from mountain peaks along the western border, to lowland areas in northeastern Alberta. It follows, then, that topographical features influence air quality - mountainous regions with little population contribute to background conditions of CO resulting in the lowest CO concentrations in the Southwest Alberta.

The main sources of CO in the atmosphere are incomplete combustion processes and photochemical oxidation of hydrocarbons (Novelli et al., 1998; Duncan et al., 2007). Hence, it is assumed that CO spatial variations in northern Alberta are associated with oil sands industrial activities and forest fires (will be discussed in section 3.5). It is reported that oil sands industry consumption of natural gas was 17x10^6 m^3/day in 2003 and is expected to increase to 40-45 million m^3/day in 2015 (NEB, 2013). However with increasing regulation of the combustion, CO is expected to decrease.

The extracted bitumen is then upgraded in upgraders located north of Fort McMurray as well as downstream industrial centers such as the industrial heartland in Fort Saskatchewan (north east Edmonton), Alberta. A small fraction of diluent used in bitumen extraction and transport is emitted to the atmosphere (Siddique et al., 2006). The diluents are mainly aromatic and aliphatic hydrocarbons (Siddique et al., 2007). As reported in earlier studies, the measured CO on 10 July 2008, as part of Arctic Research of the Composition of the Troposphere from Aircraft and Satellites (ARCTAS) mission, showed a strong correlation with alkanes, aromatics and cycloalkanes that are associated with direct emissions from the oil sands and/or diluent (Simpson et al., 2010). Furthermore, the timing, distribution of other sporadic sources such as fires, and the effects of large-scale transport have a substantial influence on the spatial discrepancies.

3.2 Time-Altitude MOPITT CO

To gain further insight about the impact of various emission sources on CO levels, temporal climatologies of 12 years for Fort McMurray (including the oil sand area), Edmonton, and Calgary areas are calculated. The monthly mean CO profiles using all the available MOPITT data between March 2002 and December 2013 are used for altitude/month contours for the two regions (Figure 5). The vertical profiles of MOPITT CO are retrieved on only 10 altitude levels (surface, 900, 800, 700, 600, 500, 400, 300, 200, 100 hPa), so levels in between have been linearly interpolated. However, earlier studies of the averaging kernels indicated that there are effectively not more than two independent pieces of information (1.4-2) in the vertical profiles retrieved by MOPITT, with more sensitivity to the middle troposphere (Deeter et al., 2007; Worden et al., 2010).

Generally, all regions demonstrate the same profile structure where CO mixing ratios are higher at low altitudes (high pressure) than high altitudes (low pressure). At Edmonton and Calgary, the vertical CO profile exhibits significant elevated levels in winter and spring, occurring in February and April with maximum mixing ratios of 175 ppb at low altitude levels (≤ 800 hPa)), while it shows minimum mixing ratios in summer. This pattern is consistent with the general seasonal cycle of CO in Northern Hemisphere (NH). Edwards et al. (2004) analyzed CO variability from the Terra MOPITT satellite in NH and their result showed peak values in the early spring due to fossil fuel burning for heating and increased power requirements. The wintertime CO emissions persist for several weeks after the emissions themselves have ceased causing high CO concentrations which are detected in early spring. In fact, the seasonal cycle of CO loading is driven primarily by the balance of emissions and photochemical production, and destruction by hydroxyl radical (OH) (Novelli et al., 1998). During the summer months under conditions of high solar illumination, OH is produced mainly through O_3 photolysis and subsequent reaction with H_2O which accounts for strongest sink of CO in summer. Thus the main (90%) CO loss is caused by OH oxidation, followed by dry deposition (Thompson, 1992).

Although both Calgary and Edmonton represent urban pollution, Calgary CO concentrations show lower values in winter. Different air masses and weather systems influence Alberta, and it is likely that these have a significant impact on air quality. Southwestern Alberta indicates a complex and non-uniform spatial pattern of chinook frequency in winter that is associated with

warmer temperature anomaly and strong westerly winds. In particular, Calgary is expected to experience Chinook winds more than Edmonton since chinook effects are strongest in southern portions of Alberta. Accordingly, Calgary is more affected by westerly winds that carry fresh air from the mountains and hence it may contribute to pollution dilution (Cullen and Marshall, 2011).

The seasonality in the Fort McMurray area has two peaks, as there is a marked increase of CO loading in summer (looks more like April and May), especially at low altitude levels (≤ 800 hPa). However, because the OH loading is higher in summer than spring, the CO peak does not persist long and declines rapidly. Simpson et al. (2011) calculated backward trajectories for ten days started on 10 July 2008 over the Athabasca surface mines (northeast Alberta) as part of the summer deployment of the ARCTAS field mission. The aircraft flew over both boreal forest and industrial land including tailings ponds and upgrader facilities. Then the aircraft flew to a clean air area further south of the oil sands area. The ten-day backward trajectories for the area south of the oil sands (by one degree) and clean areas revealed that the air masses are transported to the aircraft's pressure level from the west and not from oil sands mines to the north. Consequently, summer CO increments can be attributed to other sporadic sources such as forest fires. The forest fire emissions will be discussed in section 3.5. Furthermore the winter/spring levels over Fort McMurray area start to peak late in April and May with maximum mixing ratios of 135-155 ppb (≤ 800 hPa). Figure 5 illustrates higher CO mixing ratios at low altitude levels (≤ 800 hPa) over Edmonton and Calgary areas than Fort McMurray area, especially in winter and spring that point out the significance of the non-industrial sources (e.g. vehicle emissions) . It is reported that, CO emissions from mobile sources (e.g. transportation emissions) over Alberta in 2011 was about 900,000 tonnes which is about 60% of the total CO emissions (1.5 million tonnes) (Environment Canada, 2011).

For all locations, CO mixing ratios in spring exhibit greater values at higher altitudes (pressures less than 700 hPa) compared to other seasons. This could be attributed to seasonal variations in vertical motion or mixing, which lofts surface emissions into the upper troposphere (e.g., Duncan et al., 2007; Jiang et al., 2007; Liu et al., 2010; Livesey et al., 2013). This is further

confirmed by monthly omega averages (2002-2013) at 700 hPa (Figure 6) which indicate that the vertical mixing is more usual in May and June where omega averages range from -0.02 to -0.01.

Although monthly CO mixing ratios over Edmonton and Calgary areas are higher at lower altitudes, the CO total column monthly averages for all regions are comparable (not shown). This indicates that northern Alberta is affected more by CO plumes transported vertically above the planetary boundary layer (PBL) whereas cities such as Edmonton and Calgary are more influenced by local emissions confined in the PBL which is more pronounced over the Edmonton area.

Figure 7 shows the 12 year time series of monthly averaged CO mixing ratios (ppb) as measured by MOPITT from January 2002 to December 2013 at the ten pressure levels over Fort McMurray, Edmonton, and Calgary areas. The white intervals indicate missing data due to calibration events, instrument problems or that the pressure at that location is less than MOPITT pressure level.

Strong seasonal cycles are seen over all regions through all the years with maximum values in springtime. The magnitude of seasonal variability is not the same for all years and regions: it is more pronounced over the Edmonton and Calgary areas. CO mixing ratios show a sharp vertical gradient especially over Edmonton and Calgary areas with significantly higher values in the PBL than in the free troposphere (FT). This implies that surface emissions have a strong controlling effect on the variation of CO in the lower troposphere. This confinement of regional emissions in the lower atmosphere is likely due to subsidence prevailing over the area as indicated by positive values of vertical velocity 700 mb. On the other hand, the vertical gradient of CO mixing ratios over the Fort McMurray area is small and there are relatively high values at high altitudes (<500 hPa) which may be result of transported CO from biomass burning plumes. Furthermore, CO mixing ratios of Edmonton and Calgary areas at lower altitudes are higher than Fort McMurray area during the entire period. Additionally, the monthly average time series from 2002 to 2013 of CO mixing ratios over Fort McMurray area displays a secondary peak in summer while its magnitude varies from year to year. Summer CO episodes over Fort McMurray area could be a signature of polluted air parcels coming from biomass burning emissions. Accordingly, the impact of forest fire on CO levels is examined in section 3.4.

The inter-annual variation of CO total column is shown in Figure 8. The mean for the whole series (12-year) is calculated and then subtracted from each monthly average to show inter-annual variation. To investigate whether there is a trend; a linear regression analysis was performed to fit the observations of the monthly CO total column for Fort McMurray, Edmonton and Calgary areas. A slightly decreasing trend is identified for all regions with a declining percent (decreasing percent for the whole period) of -1 %. The seasonal variation is evident each year with small inter-annual variability. The striking feature in 2012 is the presence of an air pollution episode in summer which is more prominent over the Fort McMurray area. CO total column variation in July over Fort McMurray area shows distinct peak among all maximums with value of 2.6 $\bullet 10^{18}$ molecules cm^{-2}. Thus in section 3.5 a case study of summer 2012 is analyzed.

3.3 Comparison with MOZAIC/IAGOS Aircraft CO Profiles.

To verify MOPITT measurements, profiles of CO MOZAIC/IAGOS aircraft on descent to or ascent from Calgary airports are exploited for comparisons. The available aircraft data are between April 2009 and December 2011 with a total number of 186 profiles. Because of MOPITT's temporal resolution of 2–3 days and the blockage of clouds, there are missing data in daily CO profiles and hence only the matching MOPITT and aircraft profiles in time and location are utilized. For comparison, MOZAIC/IAGOS profiles are first interpolated to the pressure level of the corresponding MOPITT retrievals.

Since the MOPITT retrieval derives CO concentration profiles by combining its radiometric observations with a priori estimates of the vertical profile of atmospheric CO, weighted by their uncertainties. The sensitivity of the retrievals to the actual concentration profiles must be considered when conducting quantitative comparisons to independent measurements (Emmons et al., 2004; 2007). The sensitivity of the MOPITT measurements to the true CO profile is represented by averaging kernels (Deeter et al., 2003). Accordingly, the interpolated aircraft profile is transformed by applying the averaging kernel and a priori profile associated with the corresponding MOPITT retrieval using equation 1 (Emmons et al., 2009). The transformed profiles (x_{ret}) are denoted as MOZAIC/IAGOS (AK), and then they are averaged and plotted with

corresponding MOPITT retrieved vertical profiles of CO as illustrated in Figure 9a. The missing profile part above the highest altitude where MOZAIC/IAGOS measures, is estimated from the MOPITT a priori profile.

$$x_{\mathbf{ret}}=\mathbf{A}x+(\mathbf{I}-\mathbf{A})x_a$$

where $\mathbf{x_a}$ is the a priori CO profile, **A** is the averaging kernel, and **x** is the in situ CO profile.

Both aircraft and MOPITT measurements show that CO mixing ratios below 700 hPa are higher than those above 700 hPa. The vertical distributions and gradients of aircraft and MOPITT CO mixing ratios are in good agreement where their averages values match fairly well within the standard deviations at all pressure levels. However, MOPITT averages generally have positive bias in the upper troposphere where the largest differences are seen below 400 mb. This result agrees with previous validation studies which showed that there is a 14% high bias in MOPITT V5J data at 200 hPa (Deeter et al., 2013). Nevertheless, the comparison demonstrates the potential of using multispectral MOPITT CO data in estimating surface air quality (Worden et al., 2010; Deeter et al., 2011). The seasonal profiles of the available MOZAIC/IAGOS data are computed and displayed in Figure 9b. They illustrate higher concentrations in winter for all altitudes and minimum values in summer. Additionally, spring measurements exhibited relatively high mixing ratios above ~2 km. Thus the seasonal variation results are generally consistent with MOPITT results over Calgary city except that MOPITT shows the maximum in spring rather than winter. This discrepancy suggests that, winter surface emissions are more confined in the boundary layer which exacerbates the local surface pollution, resulting in high concentrations in winter. As MOPITT's sensitivity to CO is relatively low in the boundary layer (Deeter et al., 2007) surface emission may not be captured very well. Since the meteorological conditions in spring favors lofting the emissions up (warm air is of low density), retrieved MOPITT signal at mid-troposphere can capture the enhanced CO where its sensitivity is better (Hyer et al., 2007). As a result the MOPITT data show the seasonal peak in spring rather than winter. This finding suggests that the significant influence of transported emissions on CO levels. The surface seasonal variations of CO are further confirmed by analysis of ground level measurements in the next section.

3.4 Comparison with Ground Measurements

In this section we consider analysis of surface CO recorded at nine monitoring stations as the in-situ ground measurements are more sensitive to the boundary layer than the MOPITT CO. The elevation, exact location, starting date, and the status are presented in Table 2. The selected stations sample various anthropogenic sources of CO where Fort McMurray-Athabasca Valley is an industrial town and the other stations are urban sites (Edmonton and Calgary). The monthly-averaged time series of CO mixing ratio (ppb) at these stations are computed from 2000-2013 for comparison with MOPITT CO surface variability (Figure 10). The availability of CASA data differs among the stations as shown in Table 1. The MOPITT data are centred at each location in a one degree grid box.

The CO temporal evolutions from all stations reveal distinct annual and inter-annual variations with a significant declining trend. The trend is more recognizable over Edmonton and Calgary (Fig 10a and 10b) than Fort McMurray (Fig 10c) where their maximum decline percent for the whole period are 4.4%, 5.7% and 0.6%, respectively. Furthermore, the CO levels are much higher at the urban stations than the industrial one where their maximum concentrations are about 1000 ppb and 500 pbb, respectively. Comparing to MOPITT, the spatial and the temporal variations of surface CO mixing ratios also experienced higher values over Edmonton city than Fort McMurray. This finding is consistent with the results of Simpson et al. (2010) that showed relatively low emitted levels of CO throughout the mining operations (north Fort McMurray area) although the CO concentrations were 48% greater than the local background.

Additionally, it is apparent that the first 7 years (2000-2006) have larger inter-annual variations than the next years (2006-2012), especially over Edmonton and Calgary cities. In other words, the decreasing rate in the last 6 years is not as large as the first years which reflect the influence of vehicles' improvements in CO emissions (Alberta Environment, 2008). Moreover, for each city, there are discrepancies in the CO concentrations among different locations (not shown), where central and east Calgary and central and northwest Edmonton stations exhibited the greatest values (not shown). This increase could be attributed to high traffic or industrial load at these locations which imply the substantial impact of emissions sources on ambient CO levels.

The seasonal cycle of CO is evident for all years at all stations where it is characterized by a maximum in winter (December and January) and a minimum in summer (Fig. 10). It is obvious that MOPITT CO surface data capture monthly variation as ground data except at Fort McMurray 2006. However, the magnitude of the MOPITT surface values is less than ground data which could be attributed to the fact that the MOPITT surface values are is really the layer averages from the surface to the next level (e.g. 900 hPa) as well, as to low MOPITT surface sensitivity. Seasonal variations at Fort McMurray (Athabasca Valley station) (Fig. 10c) are different for the whole study period where a secondary peak in summer that is more pronounced in some years such as 2012 than in others. Interestingly, the summer 2012 peak value exceeds the winter values of the same year, where monthly CO mixing ratios in July 2012 were more than 300 ppb. Although MOPITT temporal resolution is about 3 days (Liu et al., 2005), the same feature is detected by MOPITT CO total column where the monthly July average over Fort McMurray in 2012 exceeds those of May at the same year (as shown in Figure 8). This implies the substantial impact of a non-industrial source such as forest fires, on air quality. Consequently, it is essential to analyze the biomass burning over Alberta where it is one of the major sources of CO (Morris et al., 2006).

3.5 MODIS Fire counts

To assess the impact of forest fires on CO levels, the MODIS thermal anomaly product was analyzed for 13 years (2001-2013). GIS maps were used to display the spatial distributions of active fire points using ArcGIS software version 10.1. Figure 11 illustrates the seasonal variations of fire counts for the study period over Alberta. Significant numbers of fires occurs during summer (June-August) in northern areas of Alberta extending from west to east. In the spring (February-April), large forest fires are spatially clustered in the area north of Fort McMurray as well as in central Alberta. In winter (December-February) and fall (September – November) seasons, most of the fire locations are distributed in the west and northwest areas of Alberta, especially in the fall season. Temporal analysis of fire count monthly averages for the entire period (2001-2013) demonstrates that July, June and May comprise more than 65% of the total fire occurrence where their relative frequencies are 35 %, 20%, and 8%, respectively (Fig. 12a). Thus, the period of May-July is recognized to be the main biomass burning season where the largest fires occur in Northern Alberta. High pressure subsidence (a slow, sinking motion of

high level air occurring in high pressure areas) and dry conditions were identified as the dominant conditions in this period of time (May-July) where the subsiding air is warmed by compression and becomes more stable (Skinner et al., 2002, Soja et al. 2007) which do set conditions for fires to spread and persist. Inter-annual variations of seasonal fire frequency (Fig. 12b) indicate a large variability where the total number of fire counts over Alberta increased from 1,959 in 2001 to 10,608 in 2012. A very distinct increase in fire frequency is observed in summer each year with peak number in 2012. Additionally, year 2011 exhibited an elevated number of fires in spring and summer where they exceeded 5,500 fire counts for each. The overall pattern of fires is largely consistent with the seasonal and temporal variations of MOPITT CO values of northern Alberta as well as the ground level in situ measurements at Fort McMurray station. Therefore, it is suggested that, the high CO concentrations that emerge each summer in the area around Fort McMurray (northern Alberta) are mainly caused by the biomass burning of boreal forest fires. Earlier studies pointed out the significance of biomass burning on air quality where it accounts for about 30 % of the global total CO sources (Galanter et al., 2000).

To analyze in further detail the impact of fire emissions on CO levels and their transport, the variability of fire counts during July 2012 are examined as a case study. The daily time series of fire frequency in summer 2012 (not shown) illustrates a maximum number of fires on 10 and 11 July where the fire counts exceeded 1,200 and the fire radiative power (FRP) reached 9,510 MW. Figure 13a and 13b display the MODIS Terra image combined with fire hot spots indicated by red points for 10 and 11 July 2012, respectively. It is clear that most of the red fire points are included in or headed the smoke plumes, indicating that the plumes originated from those fires.

On 10 July 2012, the air mass was transported across Alberta toward the north, then on 11 July it went from west to east at which time it splits, with part of the air mass being transported south to the Fort McMurray area. To verify the transport pathway of smoke plumes, HYSPLIT forward trajectories analyses were performed for 10 July 2012 for a 48 hour period (Figure 14a). The starting conditions for these analyses included three fire point locations chosen from the MODIS fire data. The blue circles in the trajectories represent time interval of 6 hours. Analyses were done for 500, 1,000, and 2,000 m heights, and it seems that the plumes stayed in the PBL during the first 12 hours, then all of the plumes moved upward reaching heights up to 3,000 m.

Moreover, the trajectories indicate that the air parcels traveled from northwest toward north and northeast direction which coincides with MODIS smoke plume paths (Fig.13a and 13b). Therefore, the HYSPLIT forward trajectory analysis provides evidence that some cities in Alberta could be affected by the fire emissions after a short time (24-48 h) depending on the starting plume height.

A CO total column and surface composites for July 10– 20 are displayed in Figure 13c and 13d. The plume of CO expanded across the northeast of Alberta where the CO total column and surface exceeded 3.25 x 10^18 molecules cm^{-2} and 300 ppb, respectively. Despite the limited vertical resolution of MOPITT measurements, a general enhancement of CO can be clearly seen for surface measurements where the CO mixing ratio close to fires was as high as 300 ppbv, in comparison with a CO mixing ratio of 60– 90 ppbv in the background. However, the spatial pattern of total column and surface CO are not similar where the former is more distinct in the west area of Alberta where fires originated than the latter. The location of maximum surface CO is slightly shifted to eastward from that of maximum fire counts. This is likely due to the transport of CO with the prevailing westerly winds.

Although most of the fires are originated in northwest area of Alberta (for summer 2012), MOPITT images revealed the intense CO plumes in the east which match remarkably well with MODIS and HYSPLIT trajectories. This implies the substantial influence of long range transport on CO levels where its long lifetime allows plumes with elevated CO to travel long distances affecting air quality downstream of the point source emissions. Zhao et al. (2007) indicated that a high CO episode at a remote area can result from long-range transport from active biomass burning and biofuel burning areas rather than local air pollution.

Daily time series of in-situ measurements at Athabasca Valley station for July 2012 reveals (Fig.14b) elevated CO concentrations during the intense forest fire period. Although the total number of hotspots peaked on 10 July, the enhancement of CO was found to reach the maximum value later on 12 July where it exceeded 700 ppb. This further confirms the important effect of transport on atmospheric CO values.

Generally, the in-situ measurements are in good agreement with MOPITT data, however the magnitude of in-situ measurements is higher than surface MOPITT data. The reason could be

due to the larger spatial footprint of MOPITT data (22 km×22km) while in-situ measurements represent point data. In addition, since MOPITT is not very sensitive to the CO in the boundary layer, it is possible that the sharp surface features are masked and hence the retrieved CO values in the boundary layer are lower than reality during biomass burning emissions.

4 Summary and Conclusions

This study demonstrated the potential use of MOPITT CO measurements to better understand and quantify the CO sources over Alberta. MOPITT-based climatology and inter-annual variations were conducted for 12 years (2002-2013) on spatial and temporal scales. MOPITT V5 multispectral product that uses both near-infrared and the thermal-infrared radiances for the CO retrieval were used. Available MOZAIC/IAGOS aircraft CO profiles over Calgary were used to validate MOPITT CO data. Additionally, CO ground measurements were compared to satellite data. The MODIS thermal anomaly product from 2001 to 2013 was employed to investigate the effect of seasonal variations of fires on climatological and inter-annual CO levels. To further recognize the fate and the impact of biomass burning emissions on air quality, forest fires on a sever day have been analyzed as a case study.

Seasonal climatological maps for CO total columns indicated conspicuous spatial variations in all seasons except in winter where the CO spatial variations are less prominent. High CO loadings are observed to extend from the North East to North West of Alberta, with highest values (2.5-2.75 x 10^18 molecules cm^{-2}) in spring. The CO mixing ratios at the surface level in winter and spring seasons exhibited dissimilar spatial distribution pattern where the enhancements are detected in south east Alberta (east of Edmonton city) rather than north, with mixing ratio range of 250-300 ppb. Analyzing spatial distributions of omega at the 850 mb pressure level for four seasons implied that, conditions in northeast Alberta are more favorable for up lofting while in the south subsidence of CO emissions are more likely. Thus, meteorological parameters may affect the CO spatial distribution profile where the CO total columns show remarkable enhancements in the north while the surface CO experiences high values in the south area.

The time-altitudes climatology of the CO profiles as well as the inter-annual variability are investigated for Fort McMurray, Edmonton and Calgary regions to compare impact of various

sources on CO loading. Monthly variations over Edmonton region are consistent with the general seasonal cycle of CO in Northern Hemisphere (Edwards et al., 2004) which exhibits significant enhancement in winter and spring, and minimum mixing ratios in summer. The typical seasonal CO variations over Fort McMurray area are less prominent, where there is an obvious rise of CO in summer. The same seasonal patterns are detected at various surface monitoring stations; however the magnitudes of in-situ measurements are higher. Inter-annual variations of satellite data display a slightly decreasing trend for both regions while the decline trend is more evident from ground observations, especially in the Edmonton and Calgary regions. These discrepancies (between satellite and ground data) may be explained by larger MOPITT spatial resolution and its lower sensitivity to the surface CO.

MOPITT CO profiles are validated by comparing them to the available MOZAIC/IAGOS aircraft profiles after applying averaging kernel (Emmons et al. 2009). Both vertical distributions showed good agreement within the standard deviations at all pressure levels.

Time altitude CO profile measurements over the Edmonton and Calgary regions exhibited relatively elevated CO values in the lower troposphere than the corresponding values over the Fort McMurray area. However, the total column CO values are similar. This striking feature suggests that Edmonton and Calgary regions may be blanketed by regional pollution while the Fort McMurray area (northern Alberta) may be influenced by CO plumes transported either vertically or horizontally which could be from industry and/or the biomass burning. Temporal analysis of fire frequency showed that, the main biomass burning season is from May to July where the largest fires are clustered spatially in northern and central Alberta. The spatial distributions of fires match remarkably the spatial distributions of MOPITT CO total column in spring and summer. Additionally, there is a consistency between the time evolutions of high CO episodes that are monitored by satellite and ground measurements in the Fort McMurray area and the fire frequency peak time. This finding implies that biomass burning and its transport have interesting consequences for the tropospheric CO distribution in northern Alberta, given the complex meteorology that prevails in this area.

Since 2012 depicted high fire frequency, 10 July 2012 was selected to analyze the biomass burning smoke plumes. Daily time series of ground measurements in Fort McMurray revealed elevated CO concentrations on 12 July (> 700 pbb) which is two days after peak fire frequency

(10 July). Furthermore MOPITT composite image for the fire severity period (10-20 July) displayed more intense CO plume in the east rather than west area where most of the fires originated. This result reflects the significant influence of long range transport of biomass burning emissions on CO levels which is further confirmed by MODIS smoke plume images and HYSPLIT forward trajectories.

Acknowledgment

We acknowledge the use of FIRMS data and imagery from the Land Atmosphere Near-real time Capability for EOS (LANCE) system operated by the NASA/GSFC/Earth Science Data and Information System (ESDIS) with funding provided by NASA/HQ. Also, we acknowledge the NOAA Air Resources Laboratory (ARL) for the provision of HYSPLIT transport model used in this publication. We are grateful to the satellite product developers of MOPITT CO for freely sharing the data through National Center for Atmospheric Research (NCAR) portals. The NCAR MOPITT project is supported by the National Aeronautics and Space Administration (NASA) Earth Observing System (EOS) Program. The National Center for Atmospheric Research (NCAR) is sponsored by the National Science Foundation. The authors also acknowledge the Canadian Space Agency (CSA) as they provided MOPITT instrument. Finally we are very grateful to Environment Canada and MITACS elevate program for funding this research.

5 References

Alberta Environment; Ambient Air Monitoring Methods. http://environment.alberta.ca/documents/AAMonitMethods.pdf, 2013, last access November 2013.

Alberta Environment; Oil sands, the resources. Available at http://www.oilsands.alberta.ca/FactSheets/Resource_FSht_June_2012_Online.pdf, 2012.

Amiro, B.D., J.B. Todd, B.M. Wotton, K.A. Logan, M.D. Flannigan, B.J. Stocks, J.A. Mason, D.L. Martell and K.G. Hirsch, 2001. Direct carbon emissions from Canadian forest fires, 1959–1999. Can. J. Forest. Res., 31: 512-525.

Bytnerowicz A., W. Fraczek, S. Schilling, and D. Alexander, 2010. Spatial and temporal distribution of ambient nitric acid and ammonia in the Athabasca Oil Sands Region, Alberta. J. Limnol., 69(1): 11-21.

Canadian Association of Petroleum Producers, 2012. Crude oil forecast, marketing and pipelines. http://www.strategywest.com/downloads/CAPP201206.pdf.

Colarco, P.R., M.R. Schoeberl, B.G. Doddridge, L.T. Marufu, O. Torres and E. J. Welton, 2004. Transport of smoke from Canadian forest fires to the surface near Washington, D.C.: Injection height, entrainment and optical properties. J. Geophys. Res., 109, D06203. doi:10.1029/2003JD004248.

Cullen, R.M. and S.J. Marshall, 2011. Mesoscale temperature patterns in the Rocky Mountains and foothills region of Southern Alberta. Atmos. Ocean., 49(3): 189-205. doi: 10.1080/07055900.2011.592130.

Daniel, J.S. and S. Solomon, 1998. On the climate forcing of carbon monoxide. J. Geophys. Res. 103: 13249-13260.

Deeter, M.N., D P. Edwards, J.C. Gille and J.R. Drummond, 2007. Sensitivity of MOPITT observations to carbon monoxide in the lower troposphere. J. Geophys. Res. 112: D24306. doi:10.1029/2007JD008929.

Deeter, M.N., D.P. Edwards, J.C. Gille, L.K. Emmons, G. Francis, S-P. Ho, D. Mao, D. Masters, H. Worden, J.R. Drummond and P.C. Novelli, 2010. The MOPITT version 4 CO product: Algorithm enhancements, validation, and long-term stability. J. Geophys. Res. 115: D07306. doi:10.1029/2009JD013005.

Deeter, M.N., L.K. Emmons, G.L. Francis, D.P. Edwards, J.C. Gille, J.X. Warner, B. Khattatov, D. Ziskin, J.F. Lamarque, S.P. Ho, V. Yudin, J.L. Attie, D. Packman, J. Chen, D. Mao and J.R. Drummond, 2003. Operational carbon monoxide retrieval algorithm and

selected results for the MOPITT instrument. J. Geophys. Res. 108: 4399. doi:10.1029/2002JD003186.

Deeter, M.N., S. Martínez-Alonso, D.P. Edwards, L.K. Emmons, J.C. Gille, H.M. Worden, J.V. Pittman, B.C. Daube and S.C. Wofsy, 2013. Validation of MOPITT Version 5 thermal-infrared, near-infrared, and multispectral carbon monoxide profile retrievals for 2000-2011. J. Geophys. Res. 118: 6710-6725. doi:10.1002/jgrd.50272.

Deeter, M.N., H.M. Worden, D.P. Edwards, J.C. Gille and A.E. Andrews, 2012. Evaluation of MOPITT retrievals of lower-tropospheric carbon monoxide over the United States. J. Geophys. Res. 117: D13306. doi:10.1029/2012JD017553.

Deeter, M.N., H.M. Worden, D.P. Edwards, J.C. Gille, D. Mao, and J.R. Drummond, 2011. MOPITT multispectral CO retrievals: Origins and effects of geophysical radiance errors. J. Geophys. Res. 116: D15303. doi:10.1029/2011JD015703.

Draxler, R.R. and G.D. Hess, 1998. An overview of the HYSPLIT_4 modelling system for trajectories, dispersion and deposition. Australian Meteorological Magazine 47 (4): 295-308.

Draxler, R.R. and G.D. Rolph, 2013. HYSPLIT (HYbrid Single-Particle Lagrangian Integrated Trajectory) Model access via NOAA ARL READY Website. (http://www.arl.noaa.gov/HYSPLIT.php). NOAA Air Resources Laboratory, College Park, Maryland.

Drummond, J.R., 1992. Measurements of Pollution in the Troposphere (MOPITT). IN: Gille, J.C. and G. Visconti (Eds.). The Use of EOS for Studies of Atmospheric Physics. Elsevier Science Publications, New York. pp. 77-101.

Duncan, B.N., J.A. Logan, I. Bey, I.A. Megretskaia, R.M. Yantosca, P.C. Novelli, N.B. Jones, and C.P. Rinsland, 2007. Global budget of CO, 1988–1997: Source estimates and validation with a global model. J. Geophys. Res. 112: D22301. doi:10.21029/22007JD008459.

Edwards, D.P., L.K. Emmons, D.A. Hauglustaine, D.A. Chu, J.C. Gille, Y.J. Kaufman, G. Pétron, L.N. Yurganov, L. Giglio, M.N. Deeter, V. Yudin, D.C. Ziskin, J. Warner, J-F. Lamarque, G.L. Francis, S.P. Ho, D. Mao, J. Chen, E.I. Grechko and J.R. Drummond, 2004. Observations of carbon monoxide and aerosols from the Terra satellite: Northern Hemisphere variability. J. Geophys. Res. 109: D24202. doi:10.1029/2004JD004727.

Emmons, L.K., M.N. Deeter, J.C. Gille, D.P. Edwards, J.-L Attié, J. Warner, D. Ziskin, G. Francis, B. Khattatov, V. Yudin, J.-F Lamarque, S.-P Ho, D. Mao, J.S. Chen, J. Drummond, P. Novelli, G. Sachse, M.T. Coffey, J.W. Hannigan, C. Gerbig, S. Kawakami, Y. Kondo, N. Takegawa, H. Schlager, J. Baehr, H. Zierei, 2004. Validation of Measurements of Pollution

in the Troposphere (MOPITT) CO retrievals with aircraft in situ profiles. J. Geophys. Res. 109: D03309. doi:10.1029/2003JD004101.

Emmons, L.K., D.P. Edwards, M.N. Deeter, J.C. Gille, T. Campos, P. Nédélec, P. Novelli and G. Sachse, 2009. Measurements of Pollution in the Troposphere (MOPITT) validation through 2006. Atmos Chem. Phys., 9: 1795-1803. doi:10.5194/acp-9-1795-2009.

Emmons, L.K., G.G. Pfister, D.P. Edwards, J.C. Gille, G. Sachse, D. Blake, S. Wofsy, C. Gerbig, D. Matross and P. Nédélec, 2007. Measurements of Pollution in the Troposphere (MOPITT) validation exercises during summer 2004 field campaigns over North America. J. Geophys. Res. 112: D12S02. doi:0.1029/ 2006JD007833.

Environment Canada (EC), 2012. Total air pollutants emissions for Alberta. http://www.ec.gc.ca/inrp-npri/default.asp?lang=en&n=0EC58C98#Emission_Summaries

Flannigan, M.D., K.A. Logan, B.D. Amiro, W.R. Skinner and B.J. Stocks, 2005. Future area burned in Canada. Clim. Chang., 72: 1-16.

Galanter, M., H. Levy II and G.R. Carmichael, 2000. Impacts of biomass burning on tropospheric CO, NO_x, and O_3. J. Geophys. Res. 105: 6633-6653.

Giglio, L., 2007. MODIS Collection 4 Active Fire Product User's Guide, Version 2.3. SSAI, Lanham, Maryland. http://maps.geog.umd.edu/products/MODIS_Fire_Users_Guide_2.3.pdf

Giglio, L., J. Descloitres C.O. Justice and Y.J. Kaufman, 2003. An enhanced contextual fire detection algorithm for MODIS. Remote Sens. Environ., 87: 273-282.

Gillett, N.P., A.J. Weaver, F.W. Zwiers and M.D. Flannigan, 2004. Detecting the effect of climate change on Canadian forest fires. Geophys. Res. Lett., 31: L18211. doi:10.1029/2004GL020876.

Girardin, M.P., 2007. Interannual to decadal changes in area burned in Canada from 1781 to 1982 and the relationship to Northern Hemisphere land temperatures. Global Ecol. Biogeogr., 16: 557- 566.

Howell, S.G., A.D. Clarke, S. Freitag, C.S. McNaughton, V. Kapustin, V. Brekovskikh, J-L. Jimenez and M.J. Cubison, 2014. An airborne assessment of atmospheric particulate emissions from the processing of Athabasca oil sands. Atmos Chem. Phys., 14: 5073-5087.

Hyer, E.J., D.J. Allen and E.S. Kasischke, 2007. Examining injection properties of boreal forest fires using surface and satellite measurements of CO transport. J. Geophys. Res. 112: D18307. doi:10.1029/2006JD008232.

Jacob, D.J., J.H. Crawford, H. Maring, A.D. Clarke, J.E. Dibb, L.K. Emmons, R.A. Ferrare, C.A. Hostetler, P.B. Russell, H.B. Singh, A.M. Thompson, G.E. Shaw, E. McCauley, J.R. Pederson and J.A. Fisher, 2010. The Arctic Research of the Composition of the Troposphere from Aircraft and Satellites (ARCTAS) mission: Design, execution, and first results. Atmos Chem. Phys., 10: 5191-5212. doi:10.5194/acp-10-5191-2010.

Jiang, J.H., N.J. Livesey, H. Su, L. Neary, J.C. McConnell and N.A.D. Richards, 2007. Connecting surface emissions, convective uplifting, and long-range transport of carbon monoxide in the upper troposphere: New observations from the Aura Microwave Limb Sounder. Geophys. Res. Lett., 34: L18812. doi:10.1029/2007GL030638.

Jiang, Z., D.B.A. Jones, H.M. Worden, M.N. Deeter, D.K. Henze, J. Worden, K.W. Bowman, C.A.M. Brenninkmeijer and T.J. Schuck, 2013. Impact of model errors in convective transport on CO source estimates inferred from MOPITT CO retrievals. J. Geophys. Res. 118. doi:10.1029/jgrd.50216.

Kalnay, E., M. Kanamitsu, R. Kistler, W. Collins, D. Deaven, L. Gandin, M. Iredell, S. Saha, G. White, J. Woollen, Y. Zhu, A. Leetmaa, R. Reynolds, M. Chelliah, W. Ebisuzaki, W. Higgins, J. Janowiak, K.C. Mo, C. Ropelewski, J. Wang, R. Jenne and D. Joseph, 1996. The NCEP/NCAR 40-Year Reanalysis Project. Bulletin of the American Meteorological Society 77(3): 437-471.

Kaufman, Y.J., D.D. Herring, K.J. Ranson and G.J. Collatz, 1998a. Earth Observing System AM1 mission to Earth. IEEE T. Geosci. Remote., 36(4): 1045-1055.

Kaufman, Y.J., C. Justice, L. Flynn, J. Kendall, E. Prin, L. Giglio, D.E. Ward, P. Menzel and A. Setzer, 1998b. Potential global fire monitoring from EOS‐MODIS. J. Geophys. Res. 103(D24): 32215-32338. doi:10.1029/98JD01644.

Kean, S., 2009. Eco-alchemy in Alberta. Science 326(5956): 1052-1055.

Liu, J., J.R. Drummond, Q. Li and J.C. Gille, 2005. Satellite mapping of CO emission from forest fires in Northwest America using MOPITT measurements. Remote Sens. Environ., 95(4): 502-516.

Liu, J., J.A. Logan, N.J. Livesey, I. Megretskaia, C. Carouge and P. Nedelec, 2010. Analysis of CO in the tropical troposphere using Aura satellite data and the GEOS-Chem model: Insights into transport characteristics of the GEOS meteorological products. Atmos Chem. Phys., 10: 12207-12232. doi:10.5194/acp- 10-12207-2010.

Livesey, N.J., J.A. Logan, M.L. Santee, J.W. Waters, R.M. Doherty, W.G. Read, L. Froidevaux and J.H. Jiang, 2013. Interrelated variations of O_3, CO and deep convection in the

tropical/subtropical upper troposphere observed by the Aura Microwave Limb Sounder (MLS) during 2004-2011. Atmos Chem. Phys., 13: 579-598. doi:10.5194/acp-13-579-2013.

Marenco, A., V. Thouret, P. Ned´ elec, H. Smit, M. Helten, D. Kley, F. Karcher, P. Simon, K. Law, J. Pyle, G. Poschmann, R. Von Wrede, C. Hume and T. Cook, 1998. Measurement of ozone and water vapor by Airbus in-service aircraft: The MOZAIC airborne program, an overview. J. Geophys. Res. 103: 631-642.

Marlon, J.R., P.J. Bartlein, C. Carcaillet, D.G. Gavin, S.P. Harrison, P.E. Higuera, F. Joos, M.J. Power and I.C. Prentice, 2008. Climate and human influences on global biomass burning over the past two millennia. Nat. Geosci., 1: 69-702.

Martin, R.V., 2008. Satellite remote sensing of surface air quality. Atmos. Environ., 42: 7823-7843.

Masuoka, E., A. Fleig, R.W. Wolfe and F. Patt, 1998. Key characteristics of the MODIS data products. IEEE T. Geosci. Remote 36(4): 1313-1323. doi:10.1109/36.701081.

McLinden, C.A., V. Fioletov, K.F. Boersma, N. Krotkov, C.E. Sioris, J.P. Veefkind and K. Yang, 2012. Air quality over the Canadian oil sands: A first assessment using satellite observations. Geophys. Res. Lett., 39: L04804. doi:10.1029/2011GL050273.

Morris, G.A., S. Hersey, A.M. Thompson, S. Pawson, J.E. Nielsen, P.R. Colarco, W.W. McMillan, A. Stohl, S. Turquety, J. Warner, B.J. Johnson, T.L. Kucsera, D.E. Larko, S.J. Oltmans and J.C. Witte, 2006. Alaskan and Canadian forest fires exacerbate ozone pollution over Houston, Texas, on 19 and 20 July 2004. J. Geophys. Res. 111: D24S03. doi:10.1029/2006JD007090.

National Energy Board, 2013. Canada's oil sands: Opportunities and challenges to 2015. http://www.neb.gc.ca/clf-nsi/rnrgynfmtn/nrgyrprt/lsnd/pprtntsndchllngs20152004/qapprtntsndchllngs20152004-eng.html

Nedelec, P., J-P. Cammas, V. Thouret, G. Athier, J-M. Cousin, C. Legrand, C. Abonnel, F. Lecoeur, G. Cayez and C. Marizy, 2003. An improved infrared carbon monoxide analyser for routine measurements aboard commercial Airbus aircraft: technical validation and first scientific results of the MOZAIC III programme. Atmos Chem. Phys., 3: 1551-1564. doi:10.5194/acp-3-1551-2003.

Novelli, P.C., K.A. Masarie and P.M. Lang, 1998. Distributions and recent changes in carbon monoxide in the lower troposphere. J. Geophys. Res. 103: 19015-19033.

Pétron, G., C. Granier, B. Khattotov, V. Yudin, J-F. Lamarque, L. Emmons, J. Gille and D.P. Edwards, 2004. Monthly CO surface sources inventory based on the 2000–2001 MOPITT satellite data. Geophys. Res. Lett., 31: L21107. doi: 10.1029/2004GL020560.

Percy, K.E., 2013. Geoscience of climate and energy 11. Ambient air quality and linkage to ecosystems in the Athabasca oil sands, Alberta. Geoscience Canada. http://dx.doi.org/10.12789/geocanj.2013.40.014 .

Preston, C.M. and M.W.I. Schmidt, 2006. Black (pyrogenic) carbon: A synthesis of current knowledge and uncertainties with special consideration to boreal regions. Biogeosciences 3: 397-420. http://www.biogeosciences.net/3/397/2006/.

Pfister, G. G., L. K. Emmons,1 P. G. Hess, R. Honrath, J.-F. Lamarque,1 M. Val Martin, R. C. Owen, M. A. Avery, E. V. Browell, J. S. Holloway, P. Nedelec, R. Purvis, T. B. Ryerson,4 G. W. Sachse, and H. Schlager 2006. Ozone production from the 2004 North American boreal fires, J. Geophys. Res., 111, D24S07, doi:10.1029/2006JD007695.

Ridley, B.A., S. Madronich, R.B. Chatfield, J.G. Walega, R.E. Shetter, M.A. Carroll and D.D. Montzka, 1992. Measurements and model simulations of the photostationary state during the Mauna Loa Observatory Photochemistry Experiment: Ozone production and loss rates. J. Geophys. Res. 97: 10375-10388.

Rolph, G.D., 2013. Real-time Environmental Applications and Display sYstem (READY) Website (http://www.ready.noaa.gov). NOAA Air Resources Laboratory, College Park, Maryland.

Siddique, T., P.M. Fedorak and J.M. Foght, 2006. Biodegradation of short-chain n-alkanes in oil sands tailings under methanogenic conditions. Environ. Sci. Technol., 40: 5459-5464.

Siddique, T., P.M. Fedorak, M.D. MacKinnon and J.M. Foght, 2007. Metabolism of BTEX and naphtha compounds to methane in oil sands tailings. Environ. Sci. Technol., 41: 2350-2356.

Simpson, I.J., S.K. Akagi, B. Barletta, N.J. Blake, Y. Choi, G.S. Diskin, A. Fried, H.E. Fuelberg, S. Meinardi, F.S. Rowland, S.A. Vay, A.J. Weinheimer, P.O. Wennberg, P. Wiebring, A.Wisthaler, M. Yang, R.J. Yokelson and D.R. Blake, 2011. Boreal forest fire emissions in fresh Canadian smoke plumes: C1–C10 volatile organic compounds (VOCs), CO_2, CO, NO_2, NO, HCN and CH_3CN. Atmos Chem. Phys., 11: 6445-6463. doi:10.5194/acp-11- 6445-2011.

Simpson, I.J., N.J. Blake, B. Barletta, G.S. Diskin, H.E. Fuelberg, K. Gorham, L.G. Huey, S. Meinardi, F.S. Rowland, S.A. Vay, A.J. Weinheimer, M. Yang and D.R. Blake, 2010. Characterization of trace gases measured over Alberta oil sands mining operations: 76 speciated

C2–C10 volatile organic compounds (VOCs), CO2, CH4, CO, NO, NO_2, NOy, O_3 and SO_2. Atmos Chem. Phys., 10: 11931-11954. doi:10.5194/acp-10-11931-2010.

Skinner, W.R., M.D. Flannigan, B.J. Stocks, D.M. Martell, B.M. Wotton, J.B. Todd, J.A. Mason, K.A. Logan and E.M. Bosch, 2002. A 500 mb synoptic wildland fire climatology from large Canadian forest fires, 1959–1996. Theoretical and Applied Climatology 71: 157-169.

Soja, A.J., N.M. Tchebakova, N.H.F. French, M.D. Flannigan, H.H. Shugart, B.J. Stocks, A.I. Sukhinin, E.I. Varfenova, F.S. Chapin and P.W. Stackhouse Jr, 2007. Climate induced boreal forest change: predictions versus current observations. Global Planet Change 56: 274-296.

Strausz, O., K.N. Jha and D.S. Montgomery, 1977. Chemical composition of gases in Athabasca bitumen and in low-temperature thermolysis of oil sand, asphaltene and maltene. Fuel 56: 114-120. doi:10.1016/0016-2361(77)90128-4.

Stocks, B.J., M.A. Fosberg, T.J. Lynham, L. Mearns, B.M. Wotton, Q. Yang, J.Z. Jin, K. Lawrence, G.R. Hartley, J.A. Mason, and D.W. McKenney, 1998.Climate change and forest fire potential in Russian and Canadian boreal forests. Climate Change 38(1): 1–13. doi:10.1023/A:1005306001055.

Thompson, A.M., 1992. The oxidizing capacity of the Earth's atmosphere: Probable past and future changes. Science 256: 1157-1165.

Timoney, K. and P. Lee, 2009. Does the Alberta tar sands industry pollute? The scientific evidence. The Open Conservation Biology Journal 3: 65-81.

Wood Buffalo Environmental Association, 2013. http://www.wbea.org/

Worden, H.M., M.N. Deeter, D.P. Edwards, J.C. Gille, J.R. Drummond and P.P. Nedelec, 2010. Observations of near-surface carbon monoxide from space using MOPITT multispectral retrievals. J. Geophys. Res. 115: D18314. doi: 10.1029/2010JD014242.

Zhao, C., L. Peng, X.X. Tie, Y. Lin, C. Li, X. Zheng and Y. Fang, 2007. A high CO episode of long-range transport detected by MOPITT. Water, Air and Soil Pollution 178: 207-216. doi:10.1007/sl11270-006-9191-1.

Table 1 The boundaries of study areas

Name of study area	Latitude range	Longitude range
Fort McMurray	56.0 to 58.0N	112.0 to 110.0W
Edmonton	52.0 to 54.0N	114.0 to 112.0W
Calgary	50.0 to 52.0N	115.0 to 113.0W

Table 2 Location, elevation and starting date of selected CASA monitoring stations

Name of the station	longitude	latitude	elevation	Starting date
Calgary Central 2	51.0470	-114.0747	1051.0	01/04/2008
Calgary Central	51.0471	-114.07315	1051.0	01/05/1979
Calgary East	51.0094	-114.0253	1028.0	01/08/1974
Calgary Northwest	51.0792	-114.1419	1106.0	01/08/1974
Fort McMurray-Athabasca Valley	56.7328	-111.3903	260.0	01/12/1997
Edmonton Central	53.5444	-113.4988	663.0	03/12/1976
Edmonton East	53.5481	-113.3682	679.0	01/10/1972
Edmonton Northwest	53.5942	-113.5400	679.0	12/07/1973
Edmonton South	53.5001	-113.5261	681.0	21/09/2005

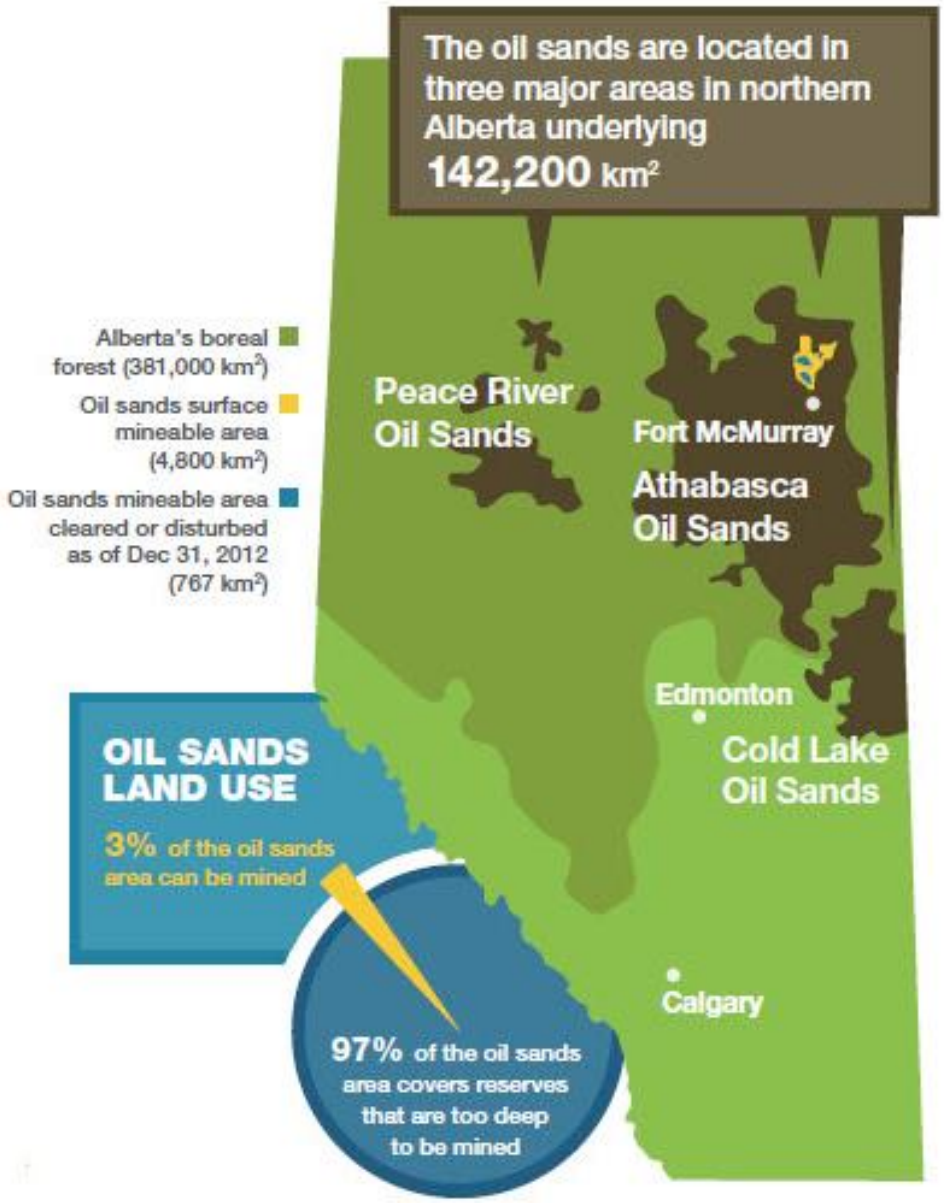

Figure 1. Alberta's oil sands deposits in the Athabasca, Peace River and Cold Lake regions (http://www.energy.alberta.ca/oilsands/791.asp.

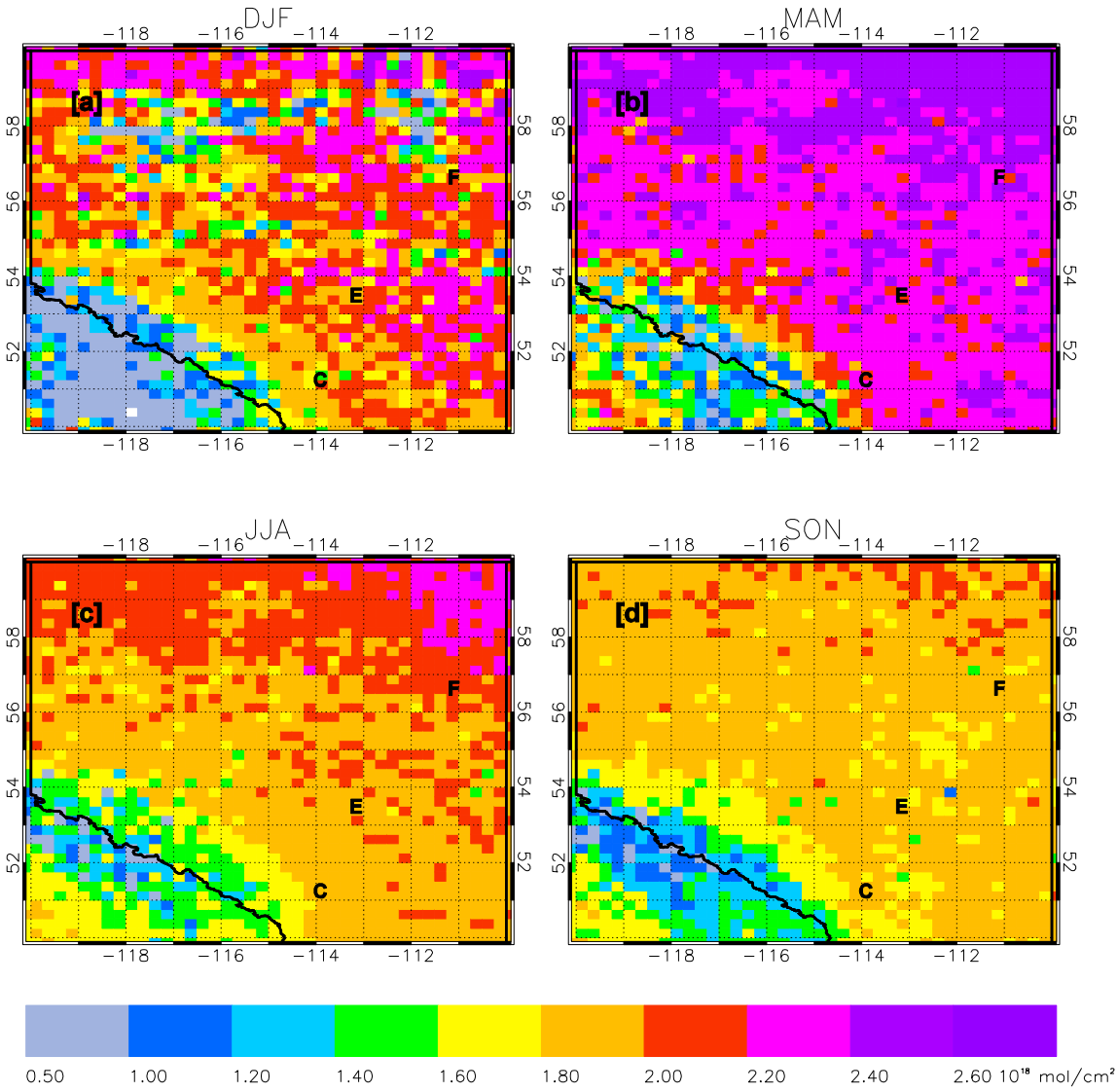

Figure 2. The MOPITT daytime CO total column measurements over Alberta for the period March 2002 to December 2013 in (a) winter, (b) spring, (c) summer and (d) fall. The symbols F, E and C represent the cities of Fort McMurray, Edmonton Calgary, respectively. Data are gridded at 0.25x0.25 degree resolution.

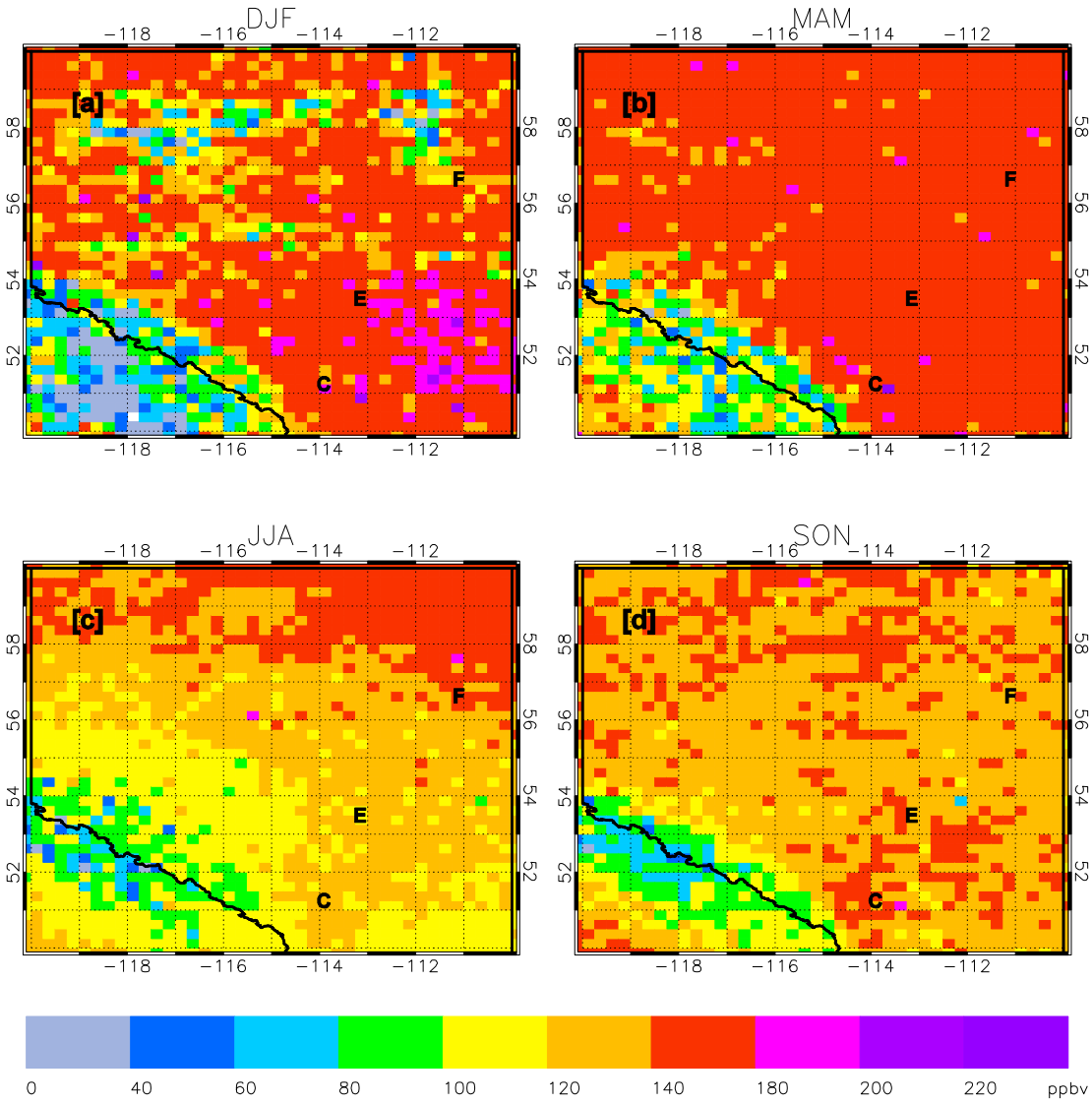

Figure 3. MOPITT daytime CO mixing ratios at the surface level over Alberta for the period March 2002 to December 2013 in (a) winter, (b) spring, (c) summer and (d) fall. The symbols F, E and C represent the cities of Fort McMurray, Edmonton and Calgary, respectively. Data are gridded at 0.25x0.25 degree resolution.

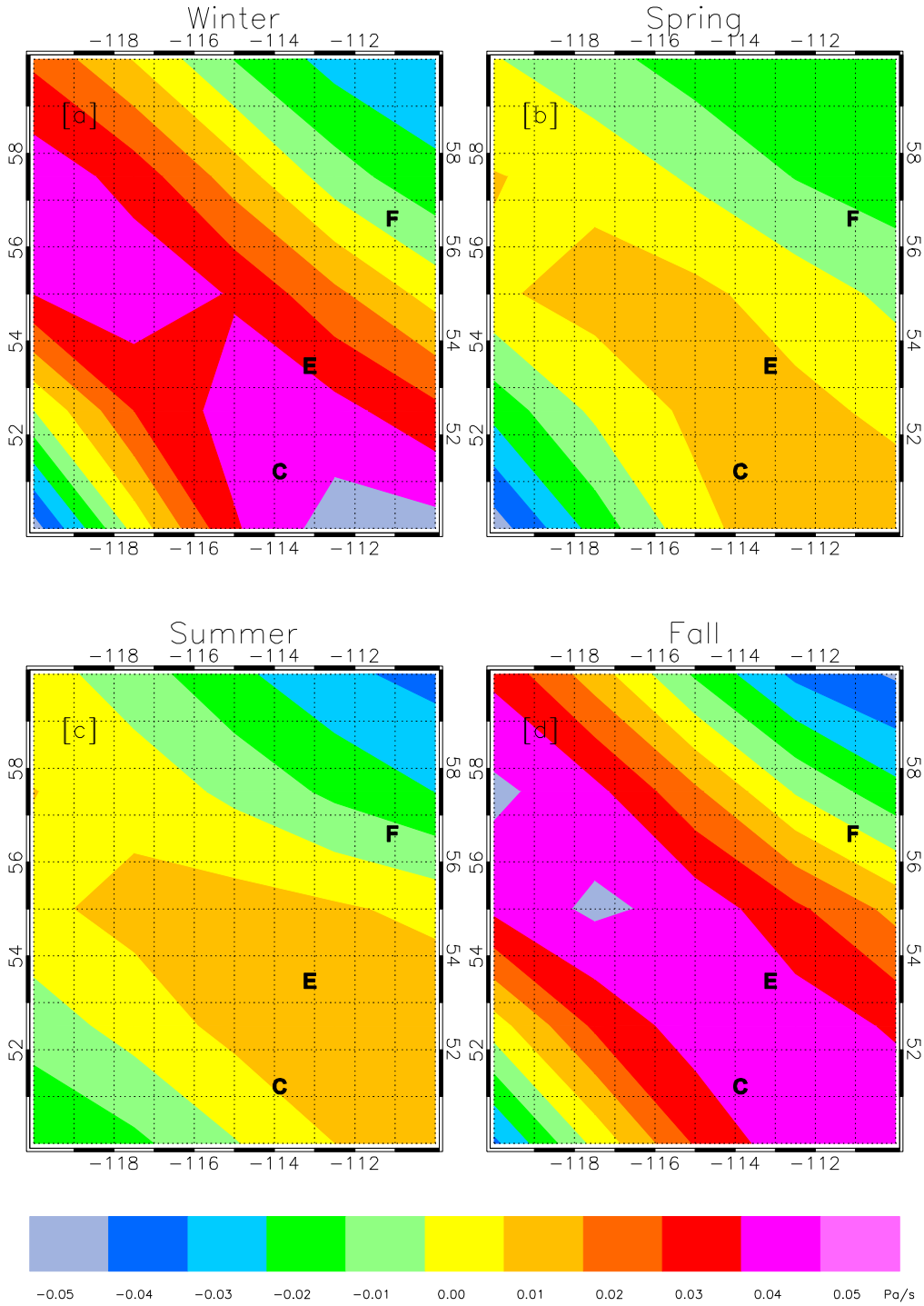

Figure 4. Spatial distributions of Omega at pressure level 850 mb for the period from 2002 to 2013 in winter (a), spring (b), summer (c), fall (d).

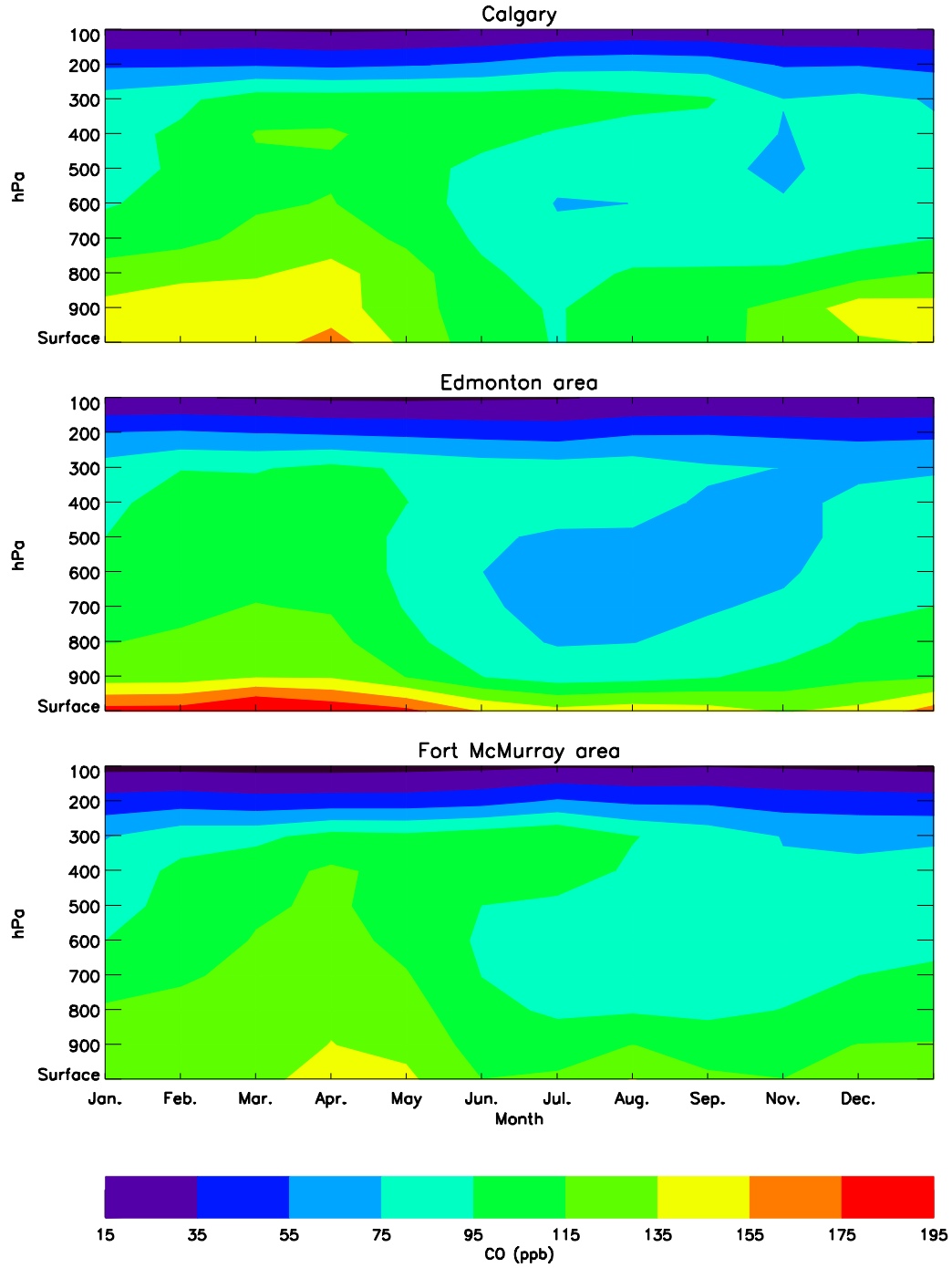

Figure 5. Climatological MOPITT CO profiles for the period March 2002 to December 2013 over Calgary, Edmonton, and Fort McMurray area.

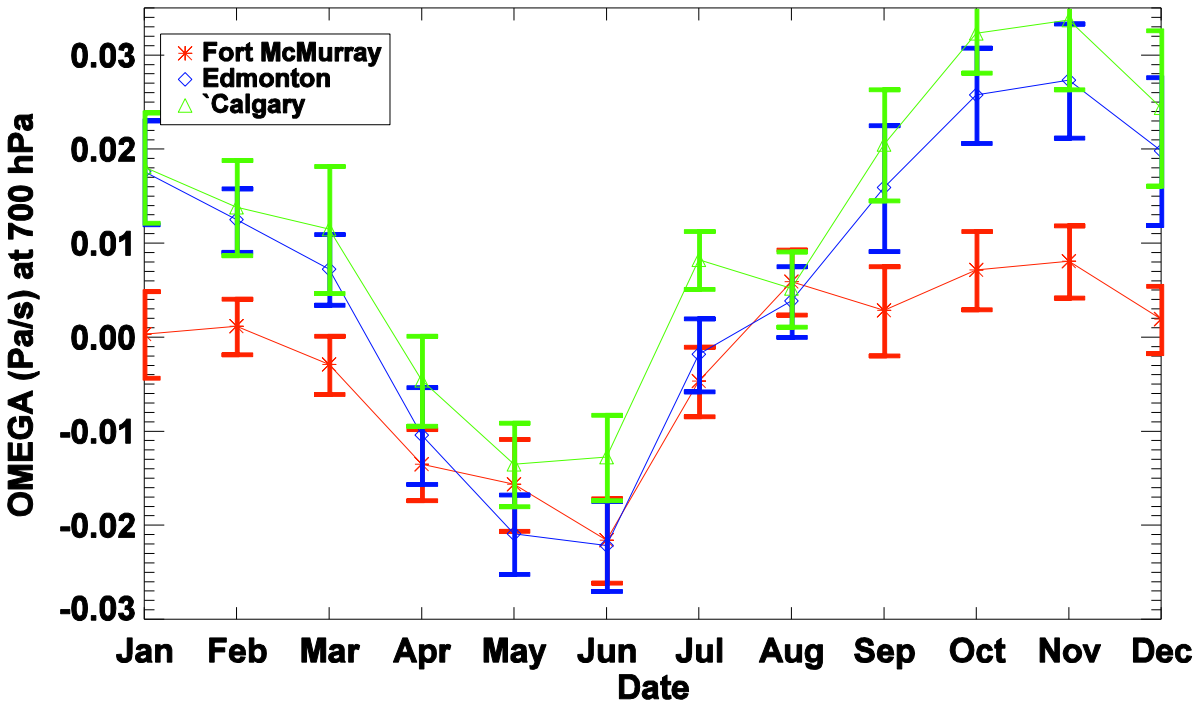

Figure 6. Omega averages at 700 hPa from 2002 to 2013.

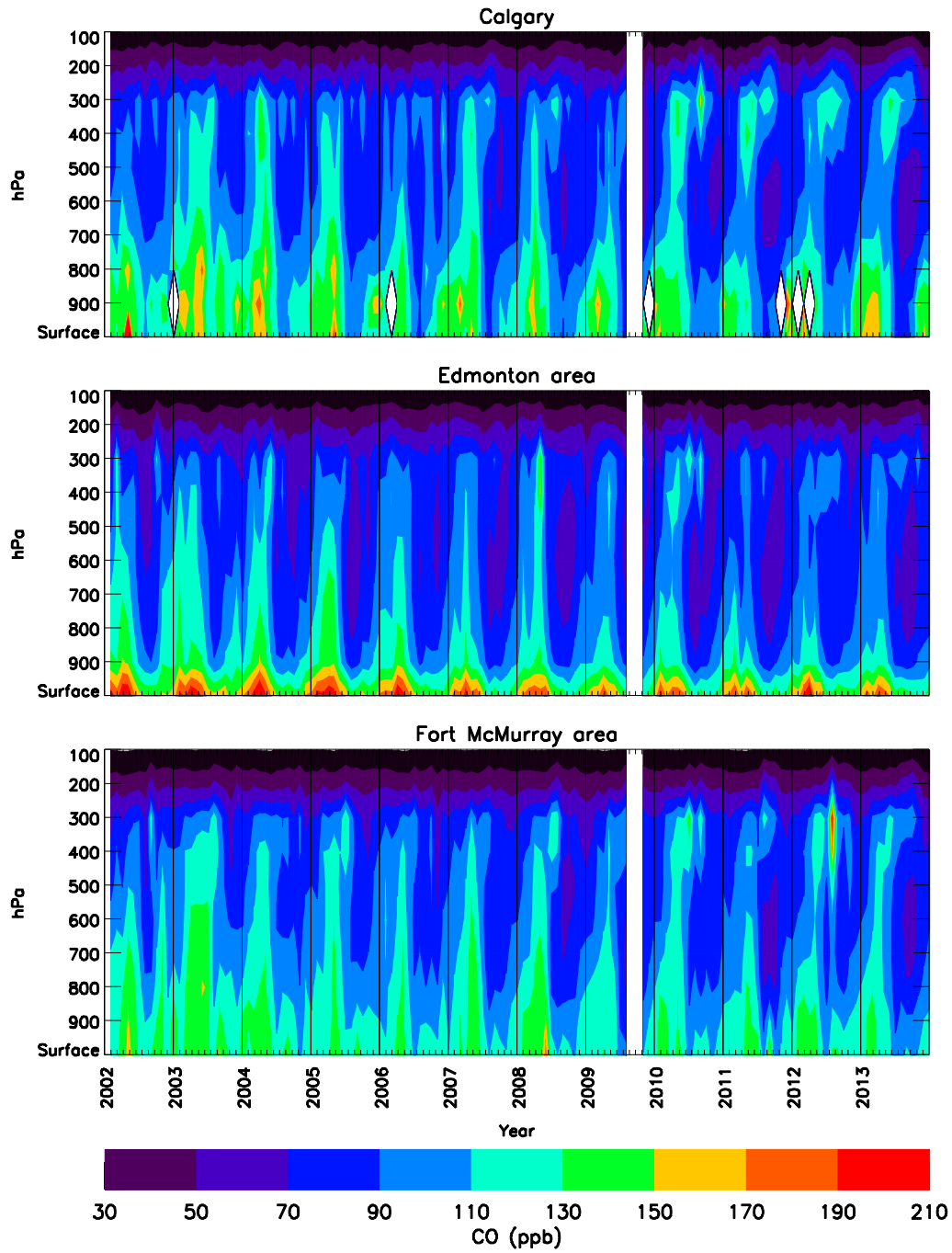

Figure 7. the 12 year inter-annual variation monthly averaged daytime MOPITT CO mixing ratios (ppb) as measured by MOPITT since January 2002 to December 2013 over Calgary, Edmonton, and Fort McMurray areas.

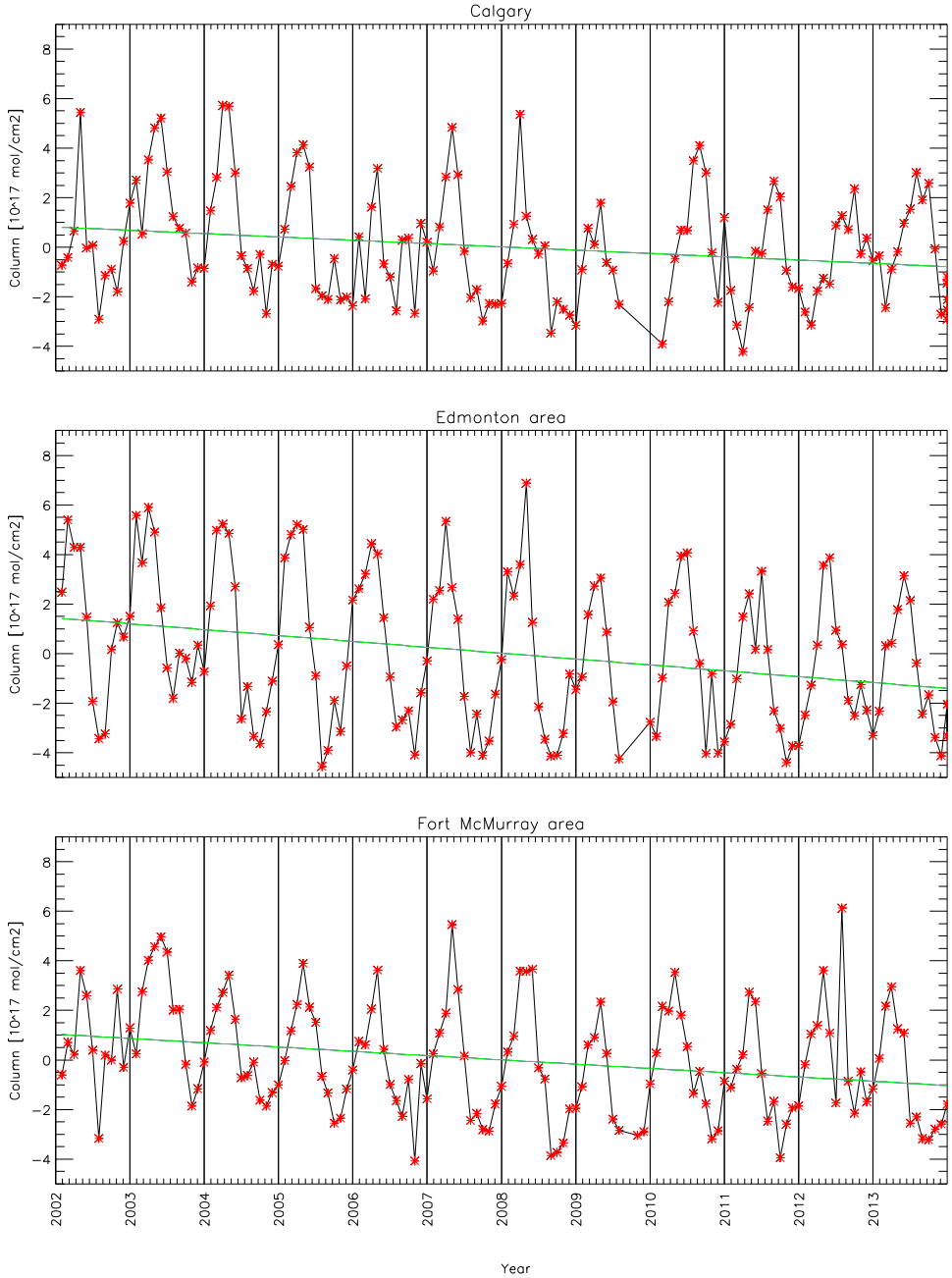

Figure 8. The 12 year inter-annual variations monthly averaged daytime MOPITT CO total column measurements for the period January 2002 to December 2013 over Calgary, Edmonton, and Fort McMurray areas.

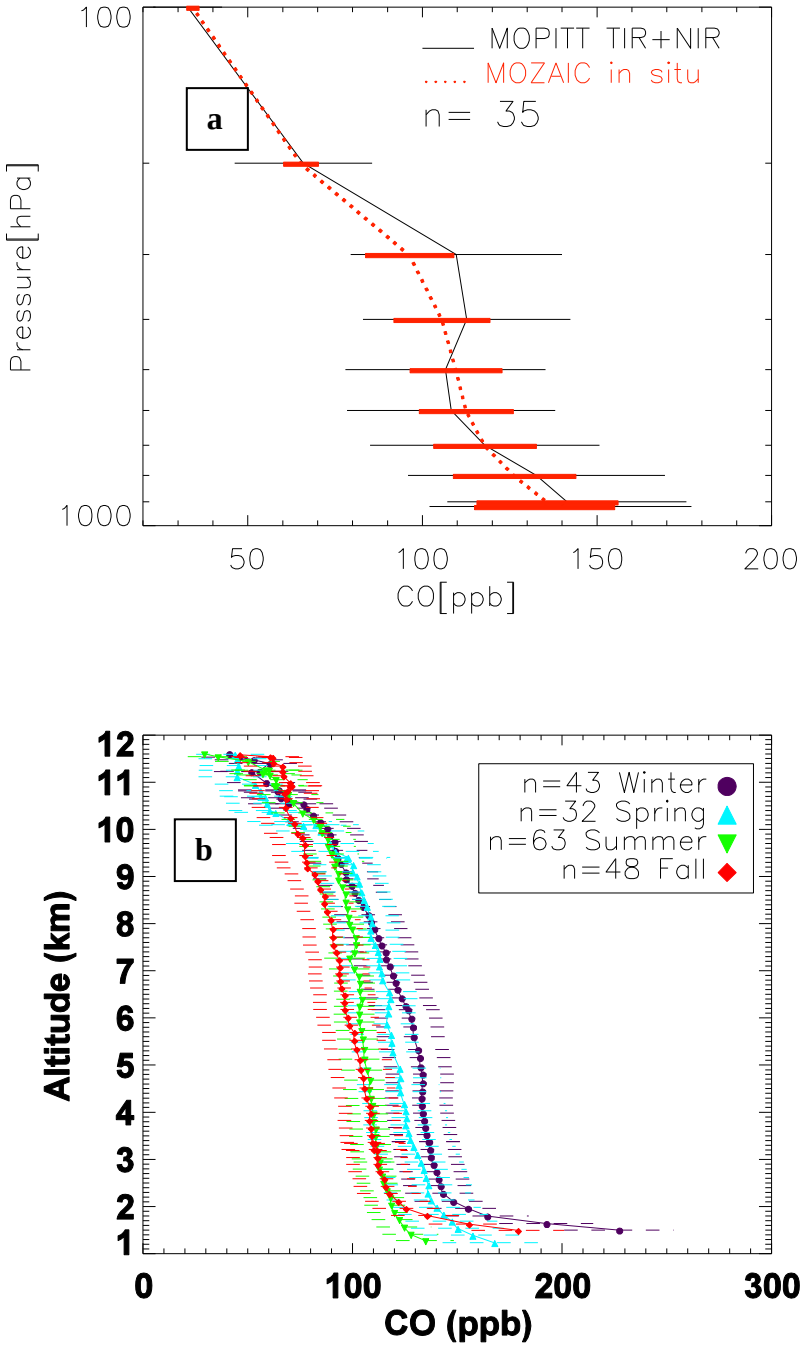

Figure 9. MOZAIC/IAGOS (AK) and the corresponding MOPITT CO profiles (a) and MOZAIC/IAGOS seasonal averages CO profiles, the horizontal bars are standard errors.

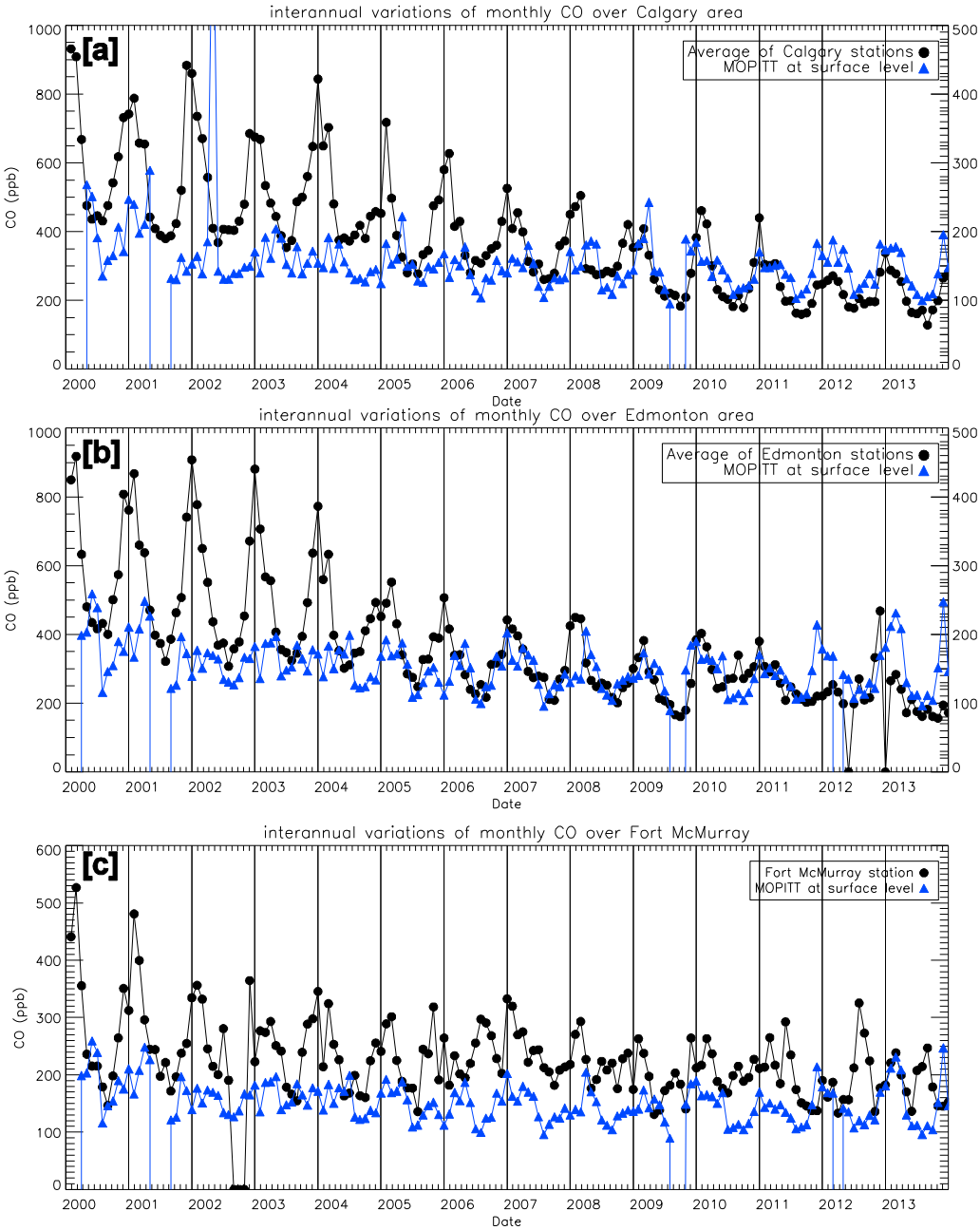

Figure 10. CASA CO in-situ measurements (left axis) and MOPITT CO at surface level (right axis) at (a) Calgary, (b) Edmonton and (c) Athabasca Valley.

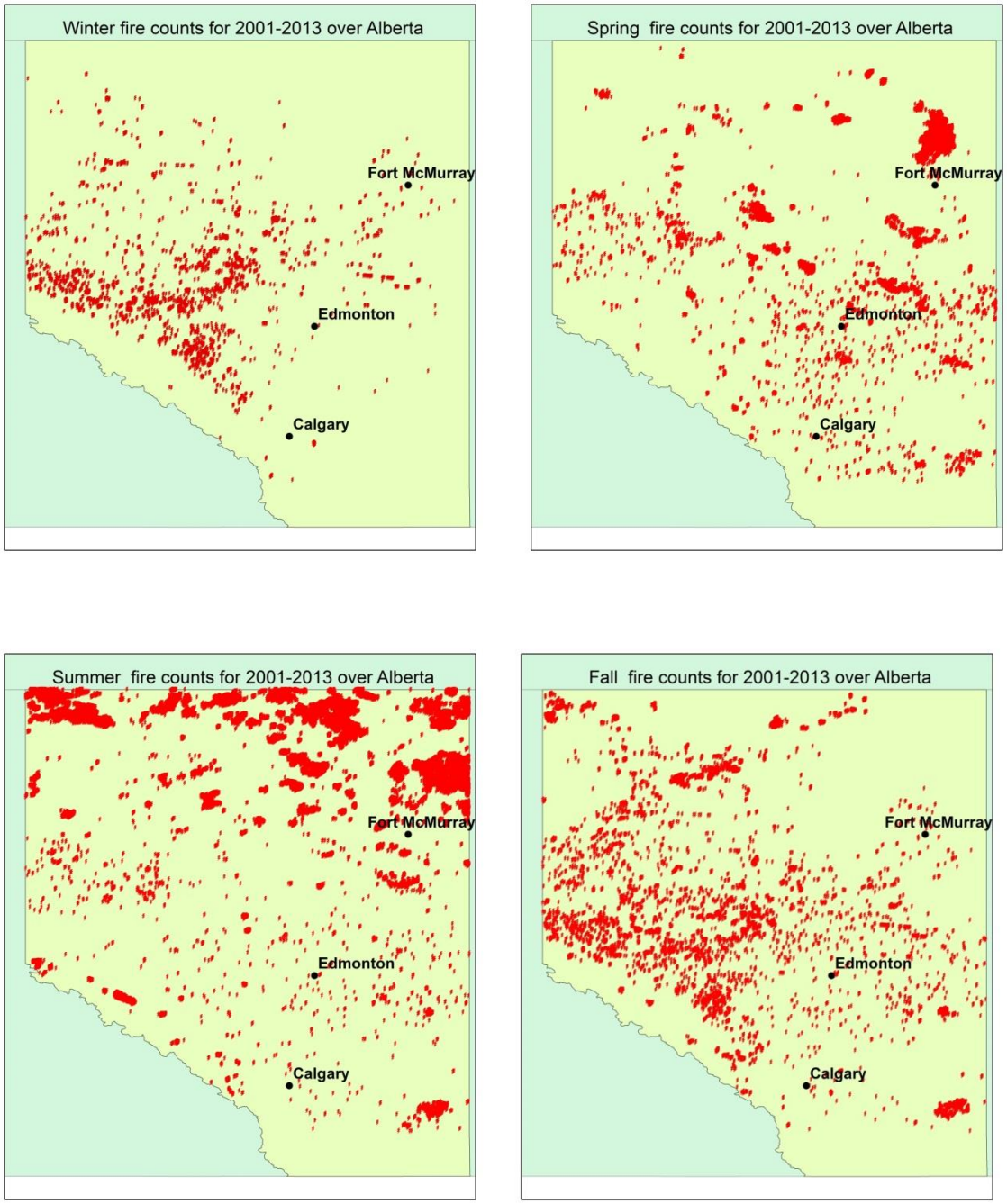

Figure 11. seasonal variations of MODIS fire counts for the study period (2001-2013) over Alberta.

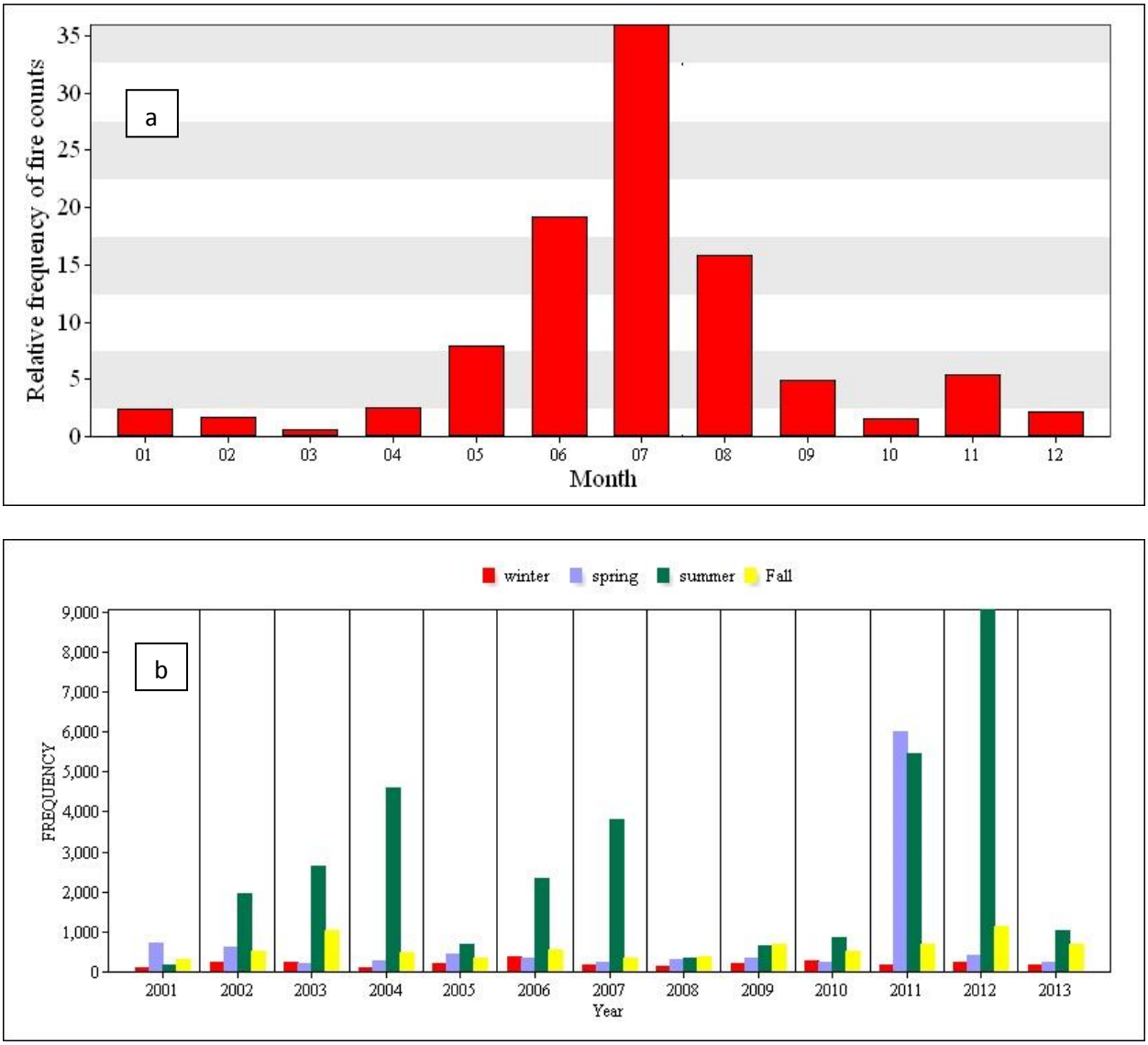

Figure 12. (a) monthly variations of MODIS fire counts for the study period (2001-2013) over Alberta, (b) Inter-annual variations of seasonal fire frequency.

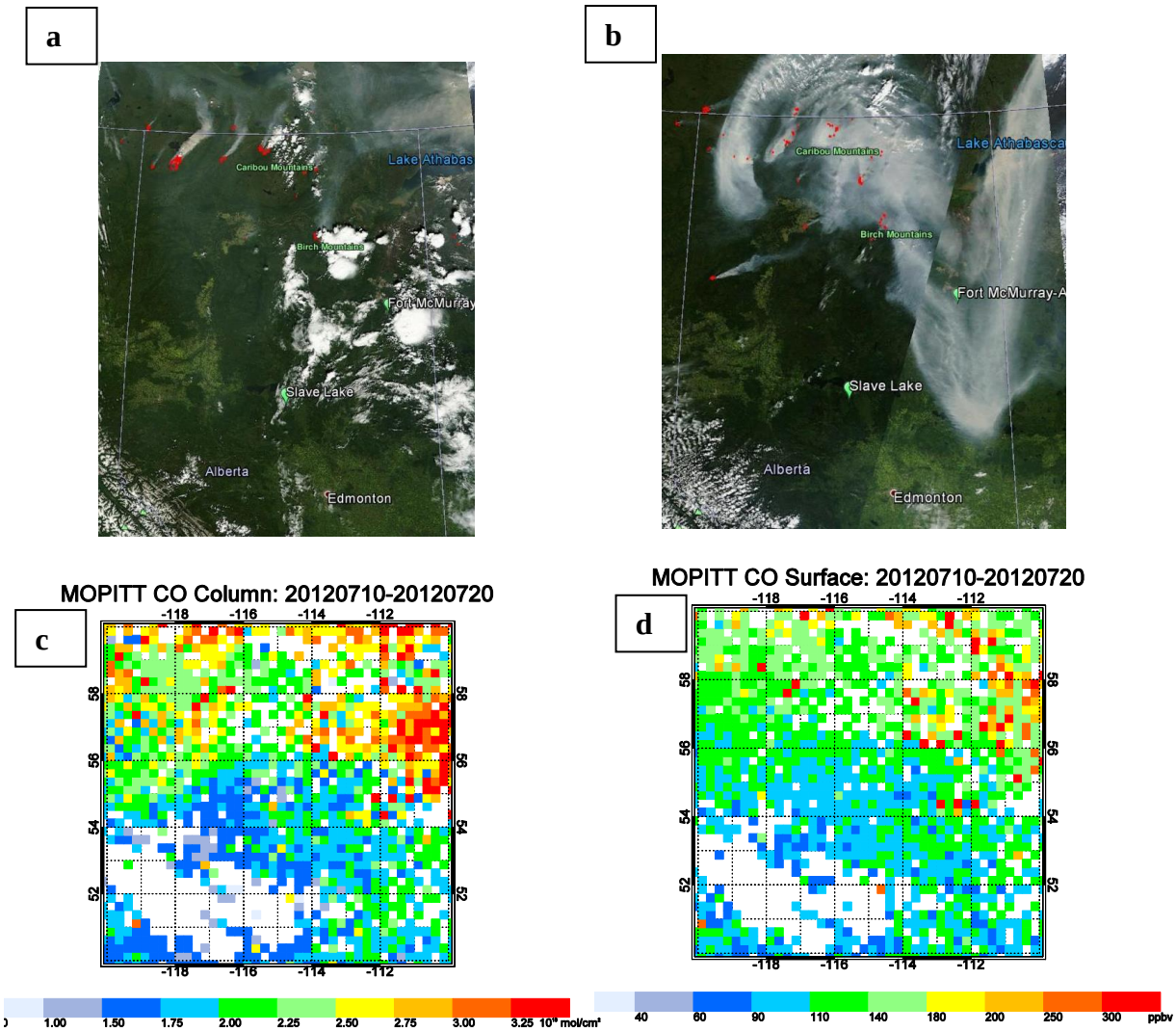

Figure 13. MODIS true image combined with fire points (red) (a) on 10 July 2012 and (b) on 11 July 2012, (c) MOPITT CO total column from 10-20 July 2012 over Alberta, (d) MOPITT surface CO from 10-20 July 2012 over Alberta.

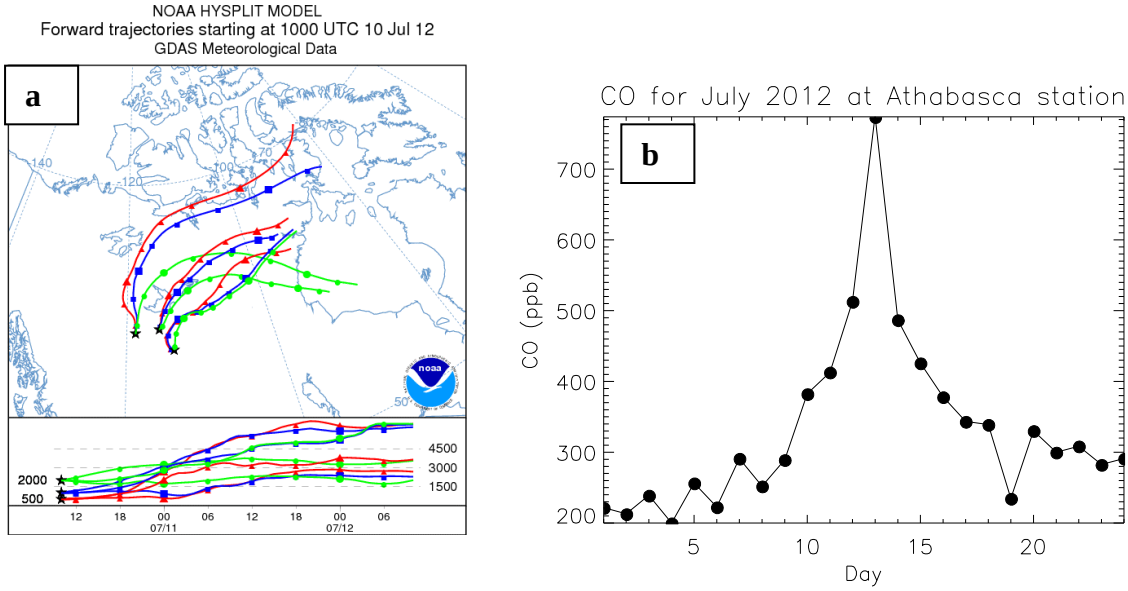

Figure 14. (a) 48 HYSPLIT forward trajectory started on 10 July 2012, and (b) daily CO at Athabasca Valley station for July 2012.